

## 7

## Wind Turbine Acoustics

**Harvey H. Hubbard**

*Distinguished Research Associate  
NASA Langley Research Center*

and

**Kevin P. Shepherd, Ph.D.**

*NASA Langley Research Center  
Hampton, Virginia*

### Introduction

Wind turbine generators, ranging in size from a few kilowatts to several megawatts, are producing electricity both singly and in wind power stations that encompass hundreds of machines. Many installations are in uninhabited areas far from established residences, and therefore there are no apparent environmental impacts in terms of noise. There is, however, the potential for situations in which the radiated noise can be heard by residents of adjacent neighborhoods, particularly those neighborhoods with low ambient noise levels. A widely publicized incident of this nature occurred with the operation of the experimental Mod-1 2-MW wind turbine, which is described in detail in [Kelley *et al.* 1985]. Pioneering studies which were conducted at the Mod-1 site on the causes and remedies of noise from wind turbines form the foundation of much of the technology described in this chapter.

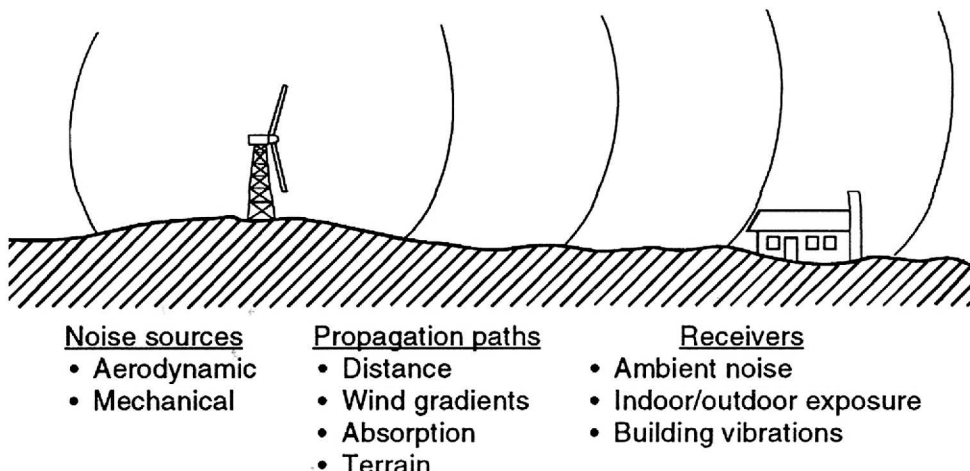


Figure 7-1. Factors contributing to wind turbine noise.

Significant factors relevant to the potential environmental impact of wind turbine noise are illustrated in Figure 7-1. All acoustic technology is built on an understanding of three primary elements: *Noise sources*, *propagation paths*, and *receivers*. The purpose, therefore, of this chapter is to describe in quantitative terms the specific wind turbine factors that characterize each of these elements. The most important of these are listed in Figure 7-1.

The noise produced by wind turbines ranges in frequency from low values that are sometimes inaudible to higher values in the normal audible range [Kelley *et al.* 1985]. Although increased distance is beneficial in reducing noise levels, the wind can enhance noise propagation in certain directions and impede it in others. A unique feature of wind turbine noise is that it can result from essentially continuous periods of daytime and nighttime operation. This is in contrast to the more common aircraft and road traffic noises that vary markedly as a function of time of day.

This chapter summarizes available information on the physical characteristics of the noise generated by wind turbines and includes example *sound pressure time histories*, *narrow-band* and *broadband frequency spectra*, and *noise radiation patterns*. Also reviewed are noise measurement standards, analysis technology, and methods for characterizing and predicting the intensity of noise from wind turbines, both singly and in clusters. Atmospheric propagation data are included that illustrate the effects of distance and the effects of refraction caused by a vertical gradient in the mean wind speed. Perception thresholds for humans are defined for both narrow-band and broadband spectra from systematic tests in the laboratory and from observations in the field. Also summarized are structural vibrations and interior sound pressure levels, which could result from the low-frequency noise excitation of buildings.

For more detailed information, a bibliography is available that lists technical papers on all aspects of wind turbine acoustics [Hubbard and Shepherd 1988].

## Characteristics of Wind Turbine Noise

Noise from wind turbines may be characterized as aerodynamic or mechanical in origin. Aerodynamic noise components are either narrow-band (containing discrete harmonics) or broadband (random) and are related closely to the geometry of the rotor, its blades, and their aerodynamic flow environments. The low-frequency, narrow-band rotational components typically occur at the blade passage frequency (the rotational frequency times the

number of blades) and integer multiples of this frequency. Of lesser importance for most configurations are mechanical noise components from operating bearings, gears, and accessories.

An example of a spectrum of wind turbine noise is shown in Figure 7-2. These data, which were measured 36 m downwind of a vertical-axis wind turbine (VAWT), show the decrease of sound pressure levels with increasing frequency (a general characteristic of wind turbines). All sound pressure levels presented in this chapter are based on root-mean-square (RMS) values of pressure; they are referenced to  $2 \times 10^{-5}$  Pa and are averaged over 30 to 180 seconds, depending on the frequency bandwidth. The spectrum generally contains broadband random noise of aerodynamic origin, although discrete components identified as mechanical noise from the gearbox are also evident. The blade passage frequency is readily apparent in the time history illustrated in Figure 7-2, as is the random nature of the emitted sounds.

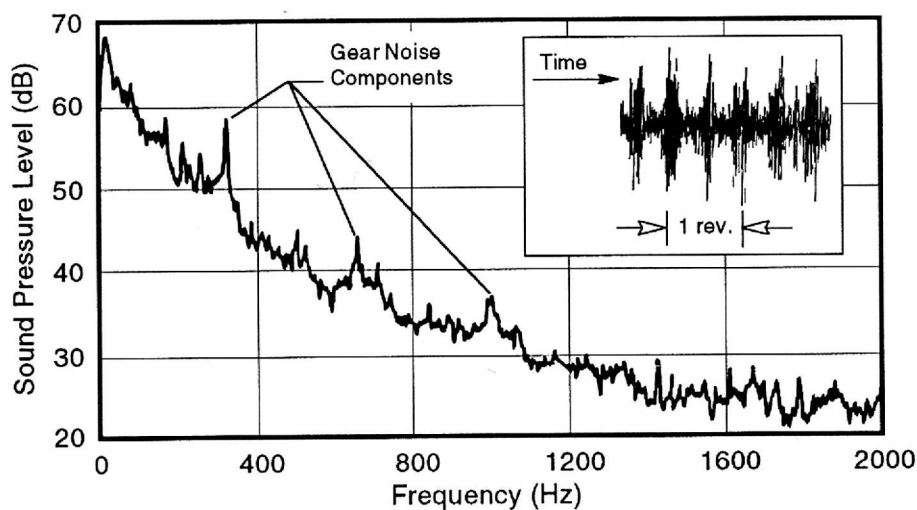


Figure 7-2. Typical narrow-band noise spectrum of a wind turbine, measured 36 m from a VAWT generating 185 kW at a wind speed of 16.5 m/s (bandwidth = 2.5 Hz)

The many analytical and experimental acoustical studies conducted on horizontal-axis wind turbines (HAWTs) indicate that for given geometrical and operational characteristics (such as power output, rotor area, and tip speed) HAWTs with downwind rotors will generate more noise than will those with upwind rotors. This is because an additional noise source in downwind rotors is introduced when the rotating blades interact with the aerodynamic wake of the supporting tower.

Because very little information on the acoustics of VAWTs is currently available, it is difficult to directly compare the noise-generation characteristics of HAWTs and VAWTs. Example VAWT spectra, levels, and directivity data are contained in Kelley, Hemphill, and Sengupta [1981] and Wehrey *et al.* [1987]. The blades of a VAWT interact with the aerodynamic wake of the rotor's central column in a manner similar to the way that a downwind HAWT rotor interacts with its tower wake, but at a greater distance relative to the column diameter. Thus, the magnitude of the noise from a VAWT caused by this interaction is expected to be less than that of an equivalent downwind HAWT rotor and greater than that of an upwind HAWT rotor. There is currently no detailed information available describing other aerodynamic noise sources associated with VAWTs. Thus, to gain an understanding of the acoustics of this type of turbine, additional studies are needed.

## Blade Impulsive Noise

Impulsive noise is often associated with downwind rotors on HAWTs; in many cases, it is the dominant noise component for that configuration. Figures 7-3(a) and (b) show example sound pressure time histories for two different HAWTs with downwind rotors [Shepherd, Willshire, and Hubbard 1988; Hubbard and Shepherd 1982]. Figure 7-3(a) relates to the 4-MW WTS-4 HAWT, with its 78.2-m-diameter rotor supported downwind of a twelve-sided shell tower. Strong impulses are superposed on less-intense broadband components. The impulse noise arises from the blade's interaction with the aerodynamic wake of the tower. As each blade traverses the tower wake, it experiences short-duration load fluctuations caused by the velocity deficiency in the wake. These load fluctuations lead directly to the radiated acoustic pulses. The acoustic pulses are all of short duration and vary in amplitude as a function of time. This variation in amplitude is believed to result from variations in the blade loadings caused by detailed differences in the time-varying structure of the aerodynamic wake [Kelley *et al.* 1985].

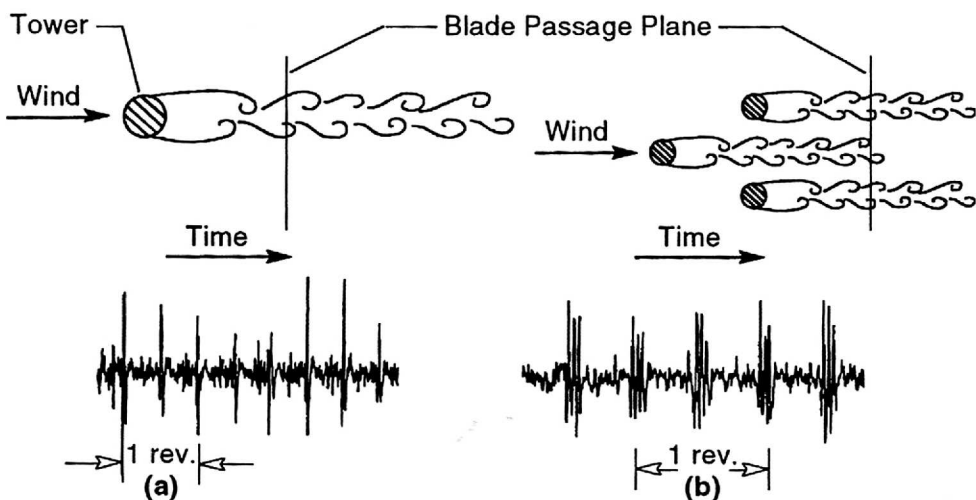


**Figure 7-3. Sound pressure time histories from two downwind-rotor HAWTs.** [Shepherd, Willshire, and Hubbard 1988; Hubbard and Shepherd 1982]. (a) 78.2-m-diameter rotor, 2 blades, 2,050-kW output, 30-rpm rotor speed, 200-m distance (b) 17.6-m-diameter rotor, 3 blades, 5-kW output, 72-rpm rotor speed, 30.5-m distance

The same phenomena, differing only in detail, are illustrated in Figure 7-3(b). These data relate to a small-scale turbine with a 17.6-m-diameter rotor supported downwind of a three-legged open truss tower [Hubbard and Shepherd 1982]. Each blade passage produces a three-peaked pulse as the blade interacts with the wakes of the three tower legs. Experimental studies by Hubbard and Shepherd [1982] and Greene [1981] showed that the character of the wake of a tower element can be altered to various degrees by adding such modifications as strakes, screens, and vanes. Because some velocity deficiency remains in the lee of the tower, it is inevitable that such modifications can ameliorate but not eliminate the impulsive noise components.

Figure 7-4 compares narrow-band spectra for upwind- and downwind-rotor HAWTs, along with their typical sound pressure time histories. The upwind HAWT is the NASA/DOE Mod-2 HAWT, 91 m in diameter and operating at a speed of 17.5 rpm. The downwind HAWT is the WTS-4 HAWT. Note that the upwind-rotor spectrum shows an

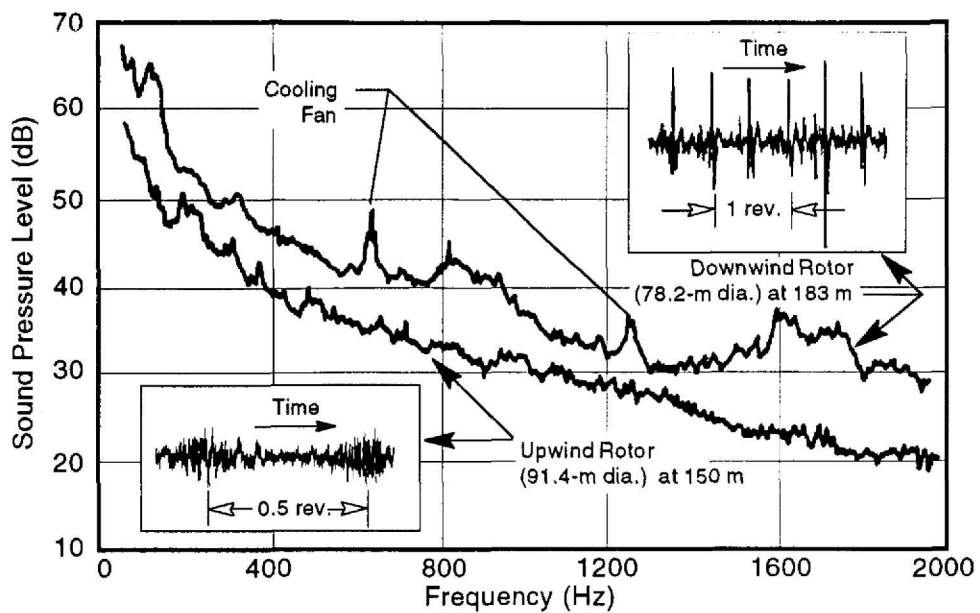


**Figure 7-4.** Narrow-band noise spectra from large-scale HAWTs with upwind and downwind rotors. (bandwidth = 2.5 Hz)

amplitude-modulated time history, but without the sharp pressure peaks that are evident for the downwind rotor. The two spectra have essentially the same shape, but the downwind-rotor spectrum shows generally higher noise levels because of its higher blade tip speed.

An expanded frequency scale is shown in Figure 7-5, in which the lower-frequency portions of the spectra in Figure 7-4 were analyzed with a narrower effective bandwidth resolution. Impulsive noises such as those illustrated in Figures 7-3(a) and 7-4 can be

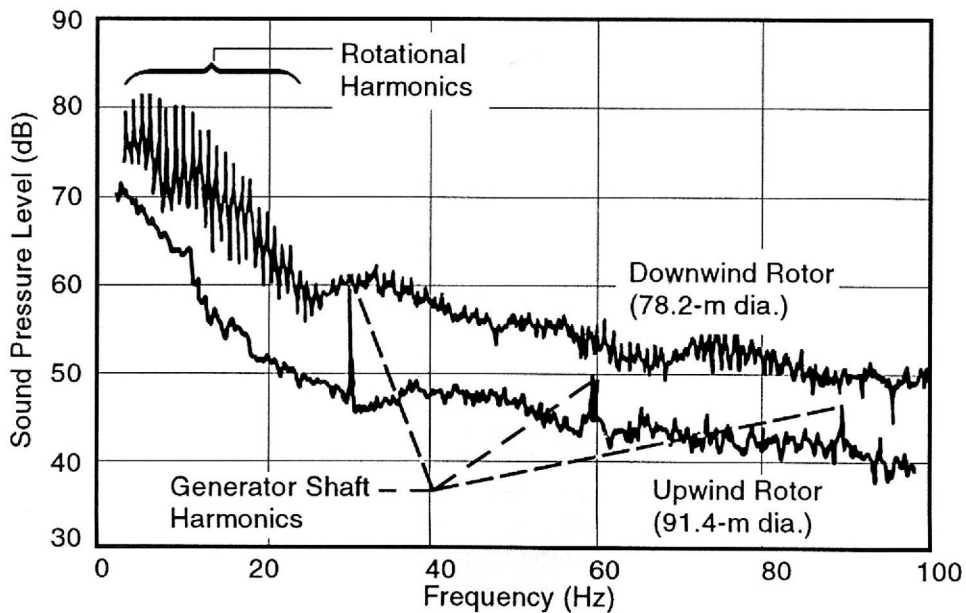


**Figure 7-5.** Low-frequency, narrow-band noise spectra from large-scale HAWTs with upwind and downwind rotors. (bandwidth = 0.25 Hz, distance = 150 m)

resolved into their *Fourier components*, which are pure tones at the blade passage frequency and integer harmonics of this frequency. These components are evident in the lower-frequency portion of the downwind-rotor spectrum of Figure 7-5, which shows identifiable rotational components out to about 30 Hz. The spectrum indicates a peak near 5 Hz and then a general decrease as the frequency increases [Shepherd and Hubbard 1983].

Figure 7-6 illustrates the nature of the noise radiation patterns for low-frequency rotational noise components. Shown are the results of simultaneous measurements of sound pressure levels at a frequency of 8 Hz; the measurements were taken at a distance of 200 m around the turbine. Acoustic radiations upwind and downwind are about equal and are greater than that in the crosswind direction. The two patterns in Figure 7-6 provide a direct comparison of measurements made at the same nominal wind conditions for daytime and nighttime operation. The nighttime levels are generally lower than the daytime levels, and the resulting radiation pattern generally appears as an acoustic dipole. The lower levels are believed to result from a different atmospheric turbulence structure during the night.

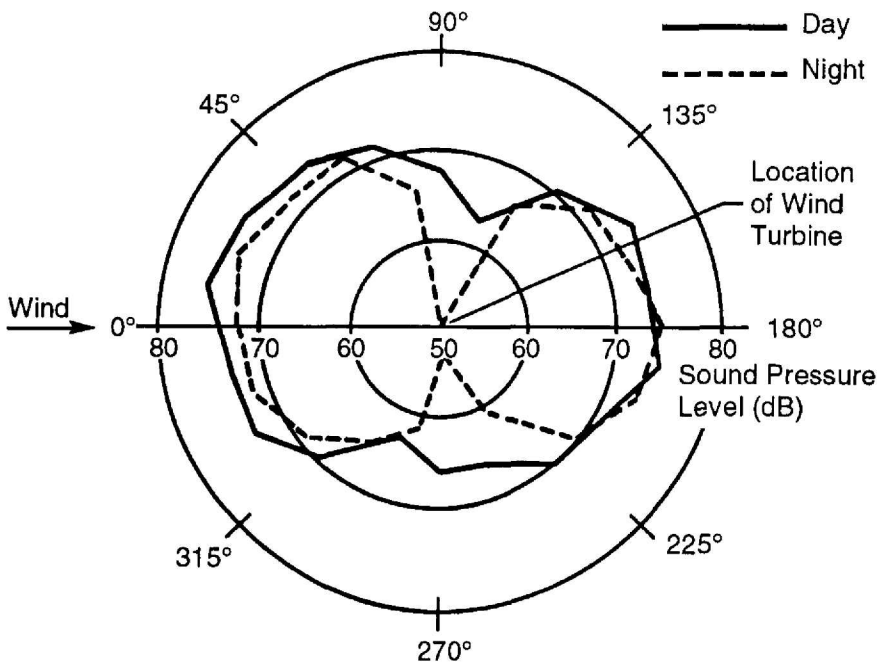


**Figure 7-6. Example radiation patterns for low-frequency rotational noise 200 m from a large-scale HAWT.** (harmonic frequency = 8 Hz, wind speed = 7.2 m/s, power = 100 kW) [Shepherd, Willshire, and Hubbard 1988]

Kelley, Hemphill, and McKenna [1982] compare characteristic low-frequency noise emissions from upwind-rotor HAWTs, downwind-rotor HAWTs, and a VAWT. These comparisons are based on joint probability distributions of octave-band sound pressure levels. The authors conclude that a downwind-rotor HAWT presents the highest probability of emitting coherent low-frequency noise, while an upwind-rotor HAWT appears to have the lowest probability of emitting such noise. The probability associated with a VAWT providing coherent noise was found to be between the two HAWT probabilities.

### Blade Broadband Noise

Broadband noise arises as the rotating blades interact with the wind inflow to the rotor. It is a significant component for all configurations of rotors, regardless of whether the low-frequency impulsive components are present. Broadband noise components are characterized by a continuous distribution of sound pressure with frequency, and they dominate a typical wind turbine acoustic spectrum at frequencies above about 100 Hz.

Example broadband-noise radiation patterns for a large-scale HAWT are shown in Figure 7-7. Data are included for one-third-octave bands with center frequencies of 100, 200, and 400 Hz. The band levels in the upwind and downwind directions are comparable but generally higher than those in the crosswind direction. The general shapes of these patterns are similar to those in Figure 7-6 for the low-frequency, rotational noise components during the daytime.

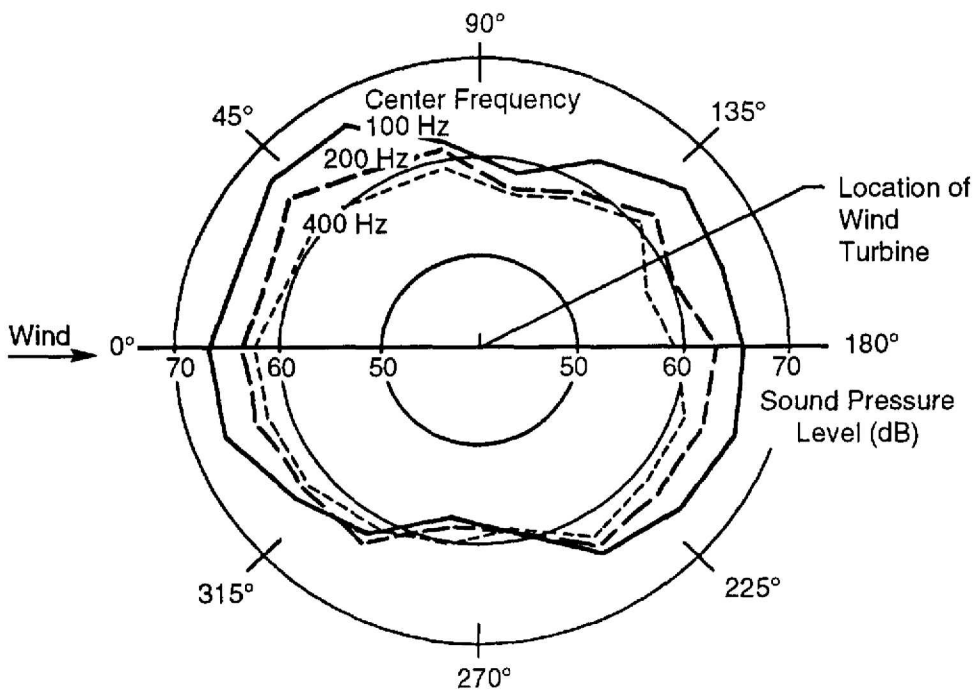


**Figure 7-7. Example radiation patterns for broadband noise 200 m from a large-scale HAWT. (one-third-octave bands, wind speed = 12.1 m/s, power = 2050 kW) [Shepherd, Willshire, and Hubbard 1988]**

The one-third-octave band spectra of Figure 7-8 were obtained for wind speeds varying by a factor of two. At lower frequencies, dominated by the rotational harmonics, the highest levels are shown to be associated with the highest wind speeds and the highest power outputs. At higher frequencies, dominated by broadband components, there is no clear trend in relation to wind speed. This result is in contrast to a scaling law given in Sutherland, Mantey, and Brown [1987], in which A-weighted sound pressure levels increase in proportion to the logarithm of the wind speed, and this contrast is verified by data from a group of several small wind turbines.

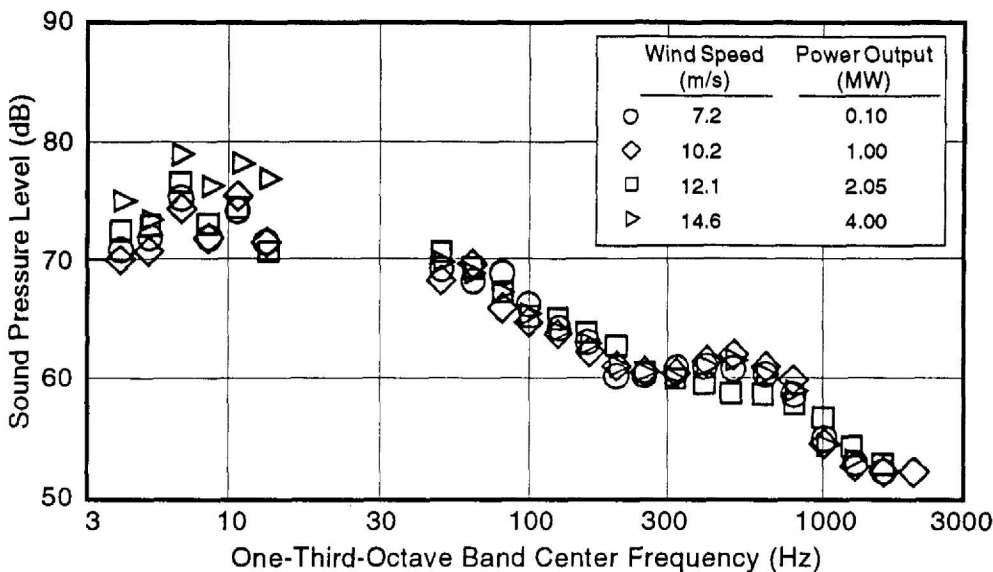


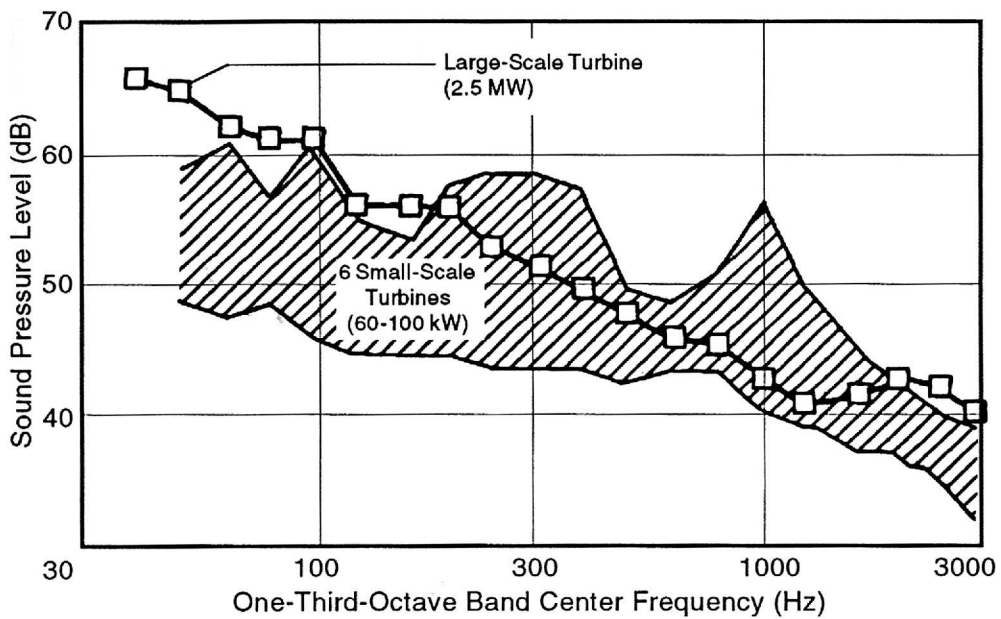
Figure 7-8. Typical variation in noise spectra with power output and wind speed, measured 200 m from a large-scale HAWT. (78.2-m diameter, downwind rotor) [Shepherd, Willshire, and Hubbard 1988]

Figure 7-8 and the upper spectrum in Figure 7-4 both represent the acoustic output of the same wind turbine. The higher sound pressure levels in Figure 7-8 are the typical result of increasing the frequency bandwidth selected for analyzing the acoustic output.

Figures 7-9 and 7-10 contain measured data for several HAWTs of various sizes and configurations [Shepherd, Willshire, and Hubbard 1988]. In Figure 7-9 [Hubbard and Shepherd 1984], measured far-field data for several upwind-rotor turbines are adjusted to a distance 2.5 rotor diameters from the base of the tower and are plotted as one-third-octave band spectra. The disk power densities (in  $\text{W/m}^2$ ) and tip speeds for all of these machines are comparable, and the spectra (adjusted for distance) are in general agreement except at the lower frequencies. Comparable data are presented in Figure 7-10 for several downwind rotors [Shepherd *et al.* 1988; Hubbard and Shepherd 1982; Shepherd and Hubbard 1981; Lunggren 1984]; the results are similar. The variations in noise levels in Figure 7-10 can be related to the variations in rotor tip speed noted in the legend. A reference gradient of -10 dB per decade is included to indicate roughly the rate at which the broadband noise levels decrease as frequencies increase.

#### Effects of HAWT Yaw Error

Horizontal-axis turbines sometimes operate such that the wind direction is not aligned with the rotor axis. The effects of nonalignment, or *yaw error*, on the generated noise have been evaluated for a large-scale HAWT with a downwind rotor. In Figure 7-11, data are shown for yaw errors of 0, 20, and 31 deg. The band levels plotted are arithmetic averages of measured values in the upwind and downwind quadrants. The obvious result is that sound pressure levels at low frequencies are reduced as yaw error increases. This would



**Figure 7-9.** Noise spectra from small- and large-scale HAWTs with upwind rotors.  
(downwind distance = 2.5 rotor diameters)

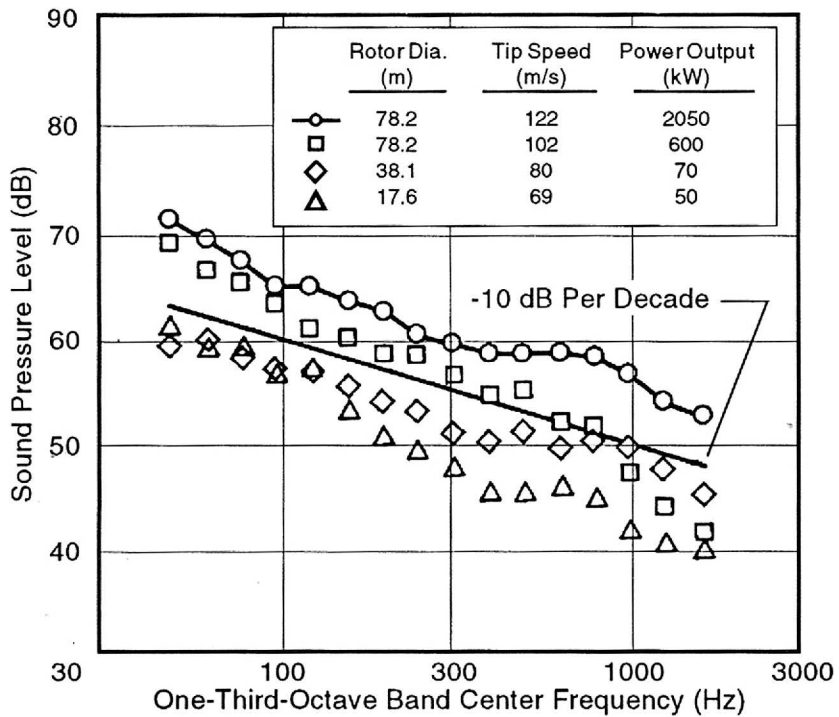


**Figure 7-10.** Noise spectra from small-, intermediate-, and large-scale HAWTs with downwind rotors. (downwind distance = 2.5 rotor diameters) [Shepherd *et al.* 1988; Lunggren 1984; Shepherd and Hubbard 1981; Hubbard and Shepherd 1982]

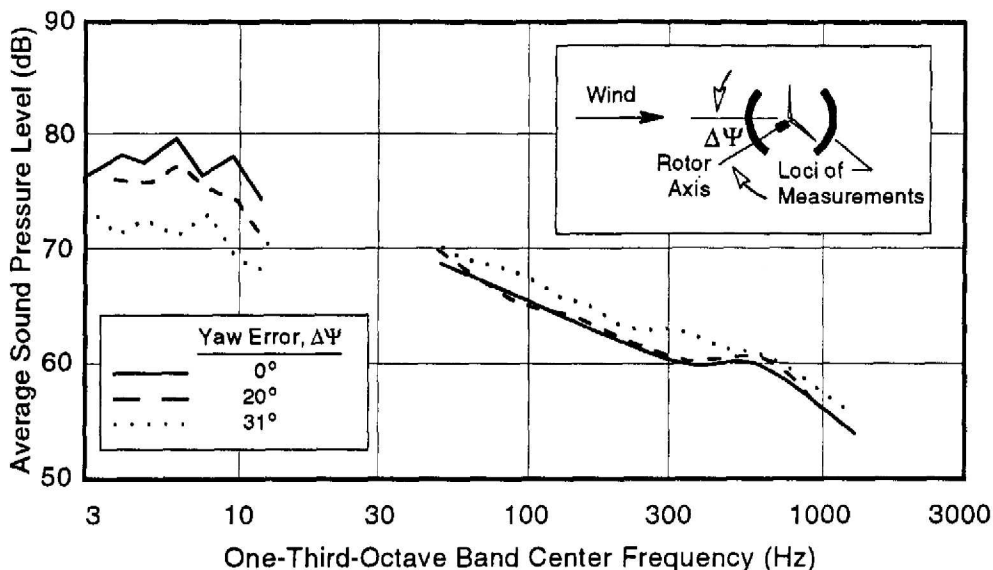


Figure 7-11. Effect of yaw error on the noise spectra of a large-scale HAWT with a downwind rotor. [Shepherd, Willshire, and Hubbard 1988]

be expected because of the reduced aerodynamic loading associated with a yaw error. At higher frequencies yaw errors cause some small increases in the sound pressure levels.

### Noise from Aileron Control Surfaces and Vortex Generators

Some experimental HAWT blades have contained *aileron*s for speed and power control. Data for two different aileron configurations are given in Shepherd and Hubbard [1984]. The unusually high noise levels observed in these tests are believed to result from the excitation of internal cavity resonances in the blades by the external flow. Well-designed aileron systems with sealed bulkheads would not have this problem.

In some situations, small tabs or *vortex generators* are installed on the low-pressure surfaces of both HAWT and VAWT blades to delay local stall and generally improve aerodynamic performance. Studies to evaluate the effects of vortex generators on noise radiations show these effects to be insignificant [Hubbard and Shepherd 1984].

### Machinery Noises

Most of the acoustic noise associated with the wind turbines studied to date has been aerodynamic in origin. Potential sources of mechanical noise, such as gears, bearings, and accessories, have not been important for large-scale HAWTs. Narrow-band analyses of noise from two large-scale HAWTs (Figures 7-4 and -5) show some cooling-fan noise and some identifiable components at the shaft speed of the generator (30 Hz) and harmonics of this speed. Because these mechanical components generally radiate in the crosswind direction and are not normally heard, they are of only secondary importance.

For some of the smaller HAWTs and some VAWTs, however, gear noise can be an important component of the total acoustic radiation. Some straightforward approaches to controlling gear noise are to include noise and vibration limits in the design specifications and to apply noise insulation around the gear box.

## Predicting Noise from a Single Wind Turbine

Extensive research studies have been conducted to predict noise from isolated airfoils, propellers, helicopter rotors, and compressors. Many of those findings have helped identify the significant noise sources of wind turbines and have helped develop methods for noise prediction. This section summarizes the technology available for predicting the sound pressure levels radiating from known sources of wind turbine noise, particularly from the aerodynamic sources which are believed to be the most important.

### Rotational Harmonics

Impulse noises like those shown in Figures 7-3 and 7-4 can be resolved into their Fourier components (Figure 7-5), which are at the blade passage frequency and its integer multiples. Acoustic pulses arise from rapidly-changing aerodynamic loads on the blades as they routinely encounter localized flow deficiencies which result in momentary fluctuations in lift and drag. Airfoil lift and drag coefficients can be transformed into thrust and torque coefficients, and these can be used to determine the unsteady blade loads associated with periodic variations in the wind velocity. These variations may occur within the tower wake, as indicated schematically in Figure 7-3, or within the swept area of the rotor, through wind shear and small-scale turbulence.

Variations in blade loading can be represented by *complex Fourier coefficients* modified by the *Sears function* to determine the effects of unsteady aerodynamics on the airfoil. The Sears function represents aerodynamic loading on a rigid airfoil passing through a sinusoidal gust [Sears 1941]. Following the model presented in Viterma [1981], a general expression for the RMS sound pressure level of the nth harmonic can be derived in the following form:

$$P_n = \frac{\sqrt{2} \sin \gamma}{4\pi R_e d} M_n^2 \sum_m e^{im(\phi - \pi/2)} J_x \left( a_m^T \cos \gamma - \frac{nB - m}{M_n} a_m^Q \right) \quad (7-1a)$$

$$M_n = nB \frac{R_e \Omega}{a_0} \quad (7-1b)$$

where

$P_n$  = RMS sound pressure for the  $n$ th harmonic ( $\text{N/m}^2$ )

$n$  = sound pressure harmonic number ( $n = 1, 2, \dots$ )

$\gamma, \phi$  = azimuth and altitude angles to the listener, respectively, referred to the rotor thrust vector (rad)

$R_e$  = effective blade radius  $\approx 0.7 \times$  tip radius,  $R$  (m)

$d$  = distance from the rotor to the listener (m)

$M_n$  = Mach Number factor for the  $n$ th harmonic

$m$  = blade loading harmonic index ( $m = \dots, -2, -1, 0, 1, 2, \dots$ )

$J_x$  = Bessel function of the first kind and of order  $x = nB - m$

$a_m^T, a_m^Q$  = complex Fourier coefficients for the thrust and torque forces acting at  $R_e$ , respectively (N)

$B$  = number of blades

$\Omega$  = rotor speed (rad/s)

$a_0$  = speed of sound (m/s)

Note that each blade loading harmonic  $m$ , caused by fluctuating air loads, gives rise to more than one sound harmonic  $n$  in the radiation field.

For the special case in which the inflow wind to the rotor disk is uniform and the listener is located in the plane of the axis (*i.e.*,  $\phi = 0$ ), Equation (7-1a) reduces to

$$P_n = \frac{\sqrt{2} \sin \gamma}{4\pi R_e d} \left( T \cos \gamma - \frac{Q a_0}{R_e^2 \Omega} \right) M_n^2 J_{nB} \quad (7-2)$$

where

$$\begin{aligned} T &= \text{rotor shaft thrust (N)} \\ Q &= \text{rotor shaft torque (N-m)} \end{aligned}$$

#### Example Rotational Noise Calculations

Examples of sound pressure levels calculated by means of Equation (7-1) for the Mod-1 HAWT are presented in Viterna [1981] and are included in Figures 7-12 and 7-13. The calculations relate to the following geometric and operating conditions:

$R = 30.5 \text{ m}$	Hub height, $H = 46 \text{ m}$
$B = 2$	Power output, $P = 1.500 \text{ kW}$
$\Omega = 34.6 \text{ rpm}$	Wind speed, $U = 13.4 \text{ m/s}$
$d = 79 \text{ m and } 945 \text{ m downwind}$	Deficit behind tower = 20% over a 20 deg sector

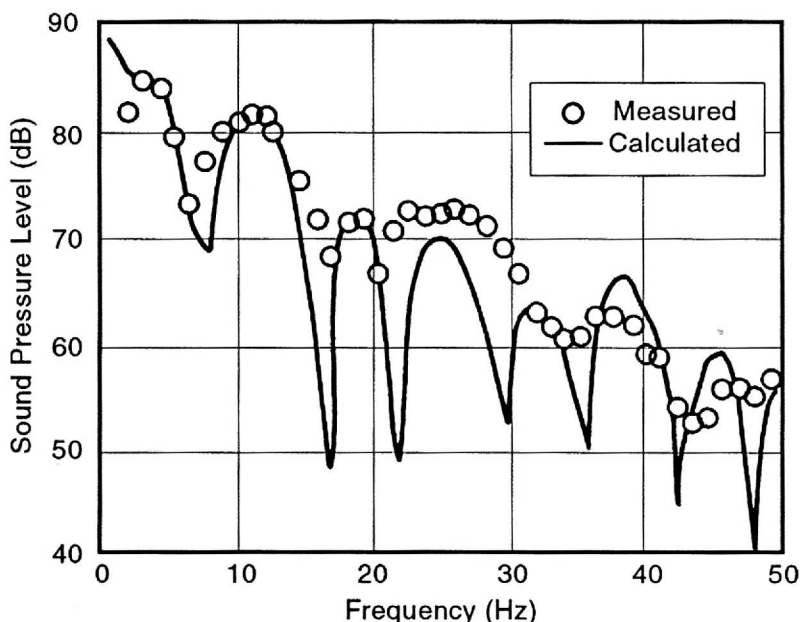
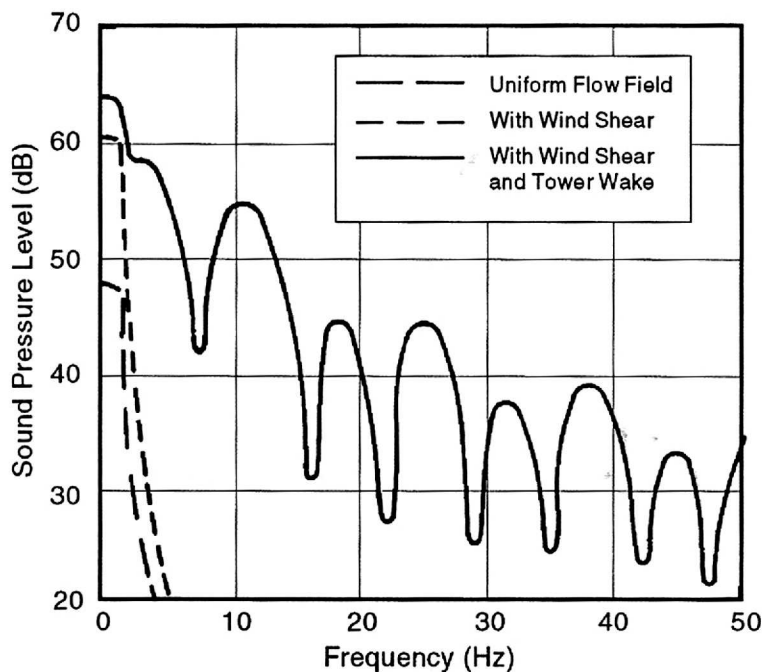


Figure 7-12. Measured and calculated rotational noise spectra 79 m downwind of the Mod-1 HAWT. (rotor diameter = 61 m, wind speed = 13.4 m/s, power output = 1,500 kW) [Viterna 1981]

Figure 7-12 compares calculated and measured sound pressure levels of the first 50 rotational harmonics for the Mod-1 downwind rotor. The calculations predict the maximum levels quite well, as well as the general shape of the spectrum. Other calculations [Viterna 1981] suggest that the maximum levels of the rotational harmonics occur in the upwind and downwind directions, while the minimum levels occur in the crosswind directions. Note that the calculation procedure presented in Equation (7-1) has been validated for the Mod-1 and WTS-4 machines. Alternative methods for predicting the magnitude of rotational harmonics are discussed, and pertinent results are presented in Kelley *et al.* [1985]; Meijer and Lindblad [1983]; Green and Hubbard [1980]; Martinez, Widnall, and Harris [1982]; George [1978]; and Lowson [1970].

Calculations made with Equation (7-2) were compared with those for a nonuniform wind inflow, and the results are shown in Figure 7-13. For a uniform flow field, the fundamental rotational harmonic is relatively strong, but all higher harmonics are weak. A similar result is obtained when the rotor operates in a shear flow that produces a once-per-revolution variation of inflow velocity at each blade. When a tower wake deficit is added, however, the levels of the higher frequencies are greatly enhanced.

These results suggest that both configuration and siting effects are significant in the rotational noise generation of wind turbines. For example, the tower wake of both VAWTs and downwind-rotor HAWTs can greatly enhance the strength of the rotational noise harmonics. Other deviations in wind inflow from a uniform velocity over the disk may also enhance the strength of the rotational harmonics for all rotor configurations. Flow deviations may be caused by the vertical wind velocity gradient in the earth's boundary layer and may be exaggerated by atmospheric turbulence or terrain features that can impose additional velocity gradients on the inflow.



**Figure 7-13. Calculated envelopes of rotational noise spectra for various wind inflow conditions 945 m downwind of the Mod-1 HAWT.** (rotor diameter = 61 m, wind speed = 13.4 m/s, power output = 1,500 kW) [Viterna 1981]

## Broadband Noise Components

Extensive research on propellers, helicopter rotors, compressors, and isolated airfoils has provided a wealth of background information and experience for predicting broadband noise for wind turbine rotors. The main noise sources have been identified, prediction techniques have been described, and comparisons have been made with available experimental data [George and Chou 1984; Glegg, Baxter, and Glendinning 1987; Grosveld 1985]. Measurements to date indicate three main sources of broadband noise are

- *aerodynamic loading fluctuations* caused by inflow turbulence interacting with the rotating blades;
- *turbulent boundary-layer flow* over the airfoil surface interacting with the blade trailing edge;
- *vortex shedding* caused by the bluntness of the trailing edge.

These sources of broadband noise are illustrated in Figure 7-14, along with their sound power dependencies, definitions of critical dimensions, and flow velocities [Grosveld 1985].

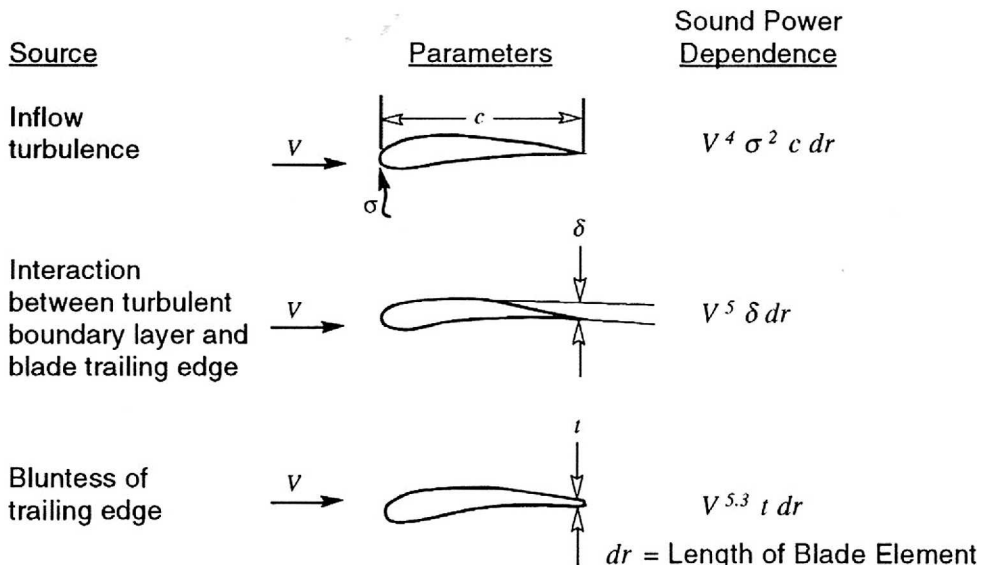


Figure 7-14. Sources of wind turbine broadband noise. [Grosveld 1985]

Another possible source of broadband noise is that of *tip vortex formation*. Based on the experimental data of isolated airfoils and rotors [George and Chou 1984; Brooks and Marcolini 1986], this source is expected to be of secondary importance relative to the three listed. However, unusual geometries, such as those associated with some tip brakes and deflected tip control surfaces, could result in significantly more radiated noise.

### Inflow Turbulence Noise

As the wind turbine blades move through the air, they encounter atmospheric turbulence that causes variations in the local angle of attack, which in turn causes fluctuations in the lift and drag forces. The length scales and intensities are a function of local atmospheric and site conditions and are different at different heights above the ground [Kelley *et al.*,

1987]. The following expression for HAWT rotor noise induced by inflow turbulence is based on the work presented in Grosveild [1985]:

$$SPL_{1/3}(f) = 10 \log_{10}[B \sin^2 \theta \rho^2 c_{0.7} R \sigma^2 V_{0.7}^4 / (d^2 a_0^2)] + K_a \quad (7-3a)$$

$$V_{0.7} = 0.7 R \Omega \quad (7-3b)$$

$$f_{peak} = S_0 V_{0.7} / (H - 0.7 R) \quad (7-4)$$

where

$SPL_{1/3}$  = one-third octave band sound pressure level (dB)

$f$  = band center frequency (Hz)

$\theta$  = angle between the hub-to-receiver line and its vertical projection in the rotor plane (rad)

$\rho$  = air density ( $\text{kg}/\text{m}^3$ )

$c_{0.7}$  = blade chord at a radius =  $0.7 R$  (m)

$\sigma^2$  = mean square of turbulence ( $\text{m}^2/\text{s}^2$ )

$V_{0.7}$  = blade forward speed at 0.7 radius (m/s)

$K_a$  = frequency-dependent scaling factor (dB; Figure 7-15)

$f_{peak}$  = frequency at which  $K_a$  is maximum (Hz; Figure 7-15)

$S_0$  = constant Strouhal number = 16.6

$H$  = hub elevation above ground (m)

A peak in the frequency domain is obtained when  $f = f_{peak}$ , which corresponds to the maximum value of  $K_a$  in Figure 7-15. Inherent in the derivation of Equation (7-3) are the assumptions that the *turbulence is isotropic* and the *atmosphere is neutrally stable* within the vertical layer occupied by the rotor. In addition, the noise source is considered to be a *point dipole* at hub height, and the wavelength of the radiated sound is much shorter

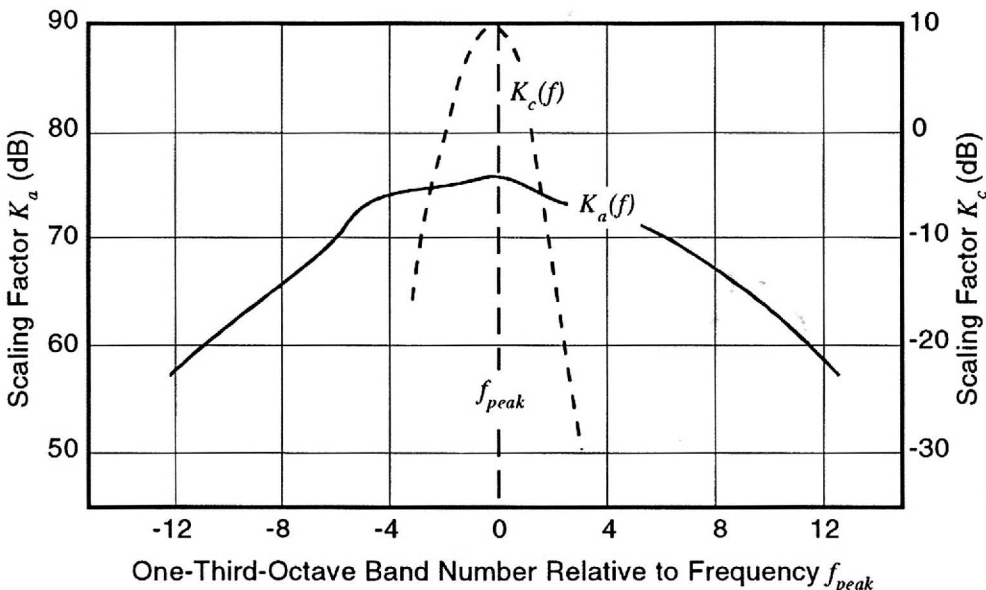


Figure 7-15. Predicted frequency-dependent scaling factors for broadband noise.

than  $d$ , the distance to the receiver. The frequency-dependent scaling factor  $K_b$ , in Figure 7-15, has been determined empirically from measured frequency spectra of rotor noise caused largely by inflow turbulence.

#### Noise from the Interaction of the Turbulent Boundary Layer and the Blade Trailing Edge

Noise is generated by the convection of the blade's attached turbulent boundary layer into the wake of the airfoil. This is a major noise source for helicopter rotors, and the studies on this subject by Schlinker and Amiet [1981] have been adapted to wind turbine rotors. The resulting expression [Grosveld 1985] for one blade airfoil is as follows:

$$SPL_{1/3}(f) = 10 \log_{10} \int_0^R \Phi_b dr + K_b \quad (7-5a)$$

$$\Phi_b = V_r^5 B D \frac{\delta}{d^2} \left( \frac{S}{S_{\max}} \right)^4 \left[ \left( \frac{S}{S_{\max}} \right)^{1.5} + 0.5 \right]^{-4} \quad (7-5b)$$

$$D = \frac{\sin^2(\theta/2)}{(1 + M \cos \theta)[1 + (M - M_c) \cos \theta]} \quad (7-5c)$$

$$M = V_r/a_0 \quad (7-5d)$$

$$\delta = 0.37c/N_R^{0.2} \quad (7-5e)$$

$$N_R = V_r c/v \quad (7-5f)$$

$$S = f\delta/V_r \quad (7-5g)$$

where

$V_r$  = resultant velocity at a blade segment (m/s)

$D$  = directivity factor

$\theta$  = angle between the segment-to-receiver line and its vertical projection in the rotor plane (rad)

$M$  = blade segment Mach number

$M_c$  = convection Mach number = 0.8  $M$

$\delta$  = boundary layer thickness (m)

$c$  = segment chord (m)

$N_R$  = segment Reynolds number

$v$  = kinematic viscosity ( $m^2/s$ )

$d$  = distance from the segment to the receiver (m)

$S$  = segment Strouhal number

$S_{\max}$  = 0.1

$dr$  = spanwise length of the blade segment (m)

$K_b$  = constant scaling factor = 5.5 dB

Sound pressure levels for the rotor are obtained by integrating contributions of all acoustic sources over the length of each blade and adding the results.

### Noise from Vortex Shedding at the Trailing Edge

Another broadband noise source is associated with vortex shedding caused by the bluntness of the trailing edge. This phenomenon is analogous to the shedding noise from wings with blunt trailing edges, as well as from flat plates, and struts [Schlinker and Amiet 1981; Brooks and Hodgson 1980]. The expression derived in Grosveld [1985] for the noise from the blunt trailing edge of one blade is

$$SPL_{1/3}(f) = 10 \log_{10} \int_0^R \Phi_c dr + K_c \quad (7-6a)$$

$$\Phi_c = \frac{B V_r^{5.3} t \sin^2(\theta/2) \sin^2 \psi}{(1 + M \cos \theta)^3 [1 + (M - M_c) \cos \theta]^2 d^2} \quad (7-6b)$$

$$f_{peak} = \frac{0.1 V_r}{t} \quad (7-7)$$

where

$t$  = trailing edge thickness (m)

$\psi$  = angle between the segment-to-receiver line and its horizontal projection in the rotor plane (rad)

$K_c$  = frequency-dependent scaling factor (dB; Figure 7-15)

The corresponding  $K_c$  has its maximum value when  $f$  reaches  $f_{peak}$  (Figure 7-15). Once again, sound pressure levels for the rotor are obtained by integrating the contributions of all acoustic sources over the length of each blade and adding the results.

### Example Calculations and Measurements of HAWT Broadband Noise

Figure 7-16 illustrates the relative contributions of the broadband noise components calculated by using Equations (7-3) to (7-7) for a large-scale HAWT with an upwind rotor. The calculations are in the form of one-third-octave band spectra for each of the broadband components identified. Also included is the summation of the components. As shown in Figure 7-16, inflow turbulence contributes noise over the whole frequency range and dominates the spectrum at frequencies below about 500 Hz. Effects of boundary-layer interaction also contribute noise over a wide frequency range but are most significant at higher frequencies. On the other hand, the noise spectrum of the trailing edge wake is sharply peaked; the maximum for the example turbine is near 1,250 Hz.

Figure 7-17 presents sound pressure levels calculated by using the methods of Grosveld and compares them with acoustic far-field measurements for a large, upwind-rotor HAWT and two different downwind-rotor HAWTs. Good agreement is shown in all cases. Note that the validation of Equations (7-3) to (7-7) has been limited to acoustic radiation in the upwind and downwind directions only.

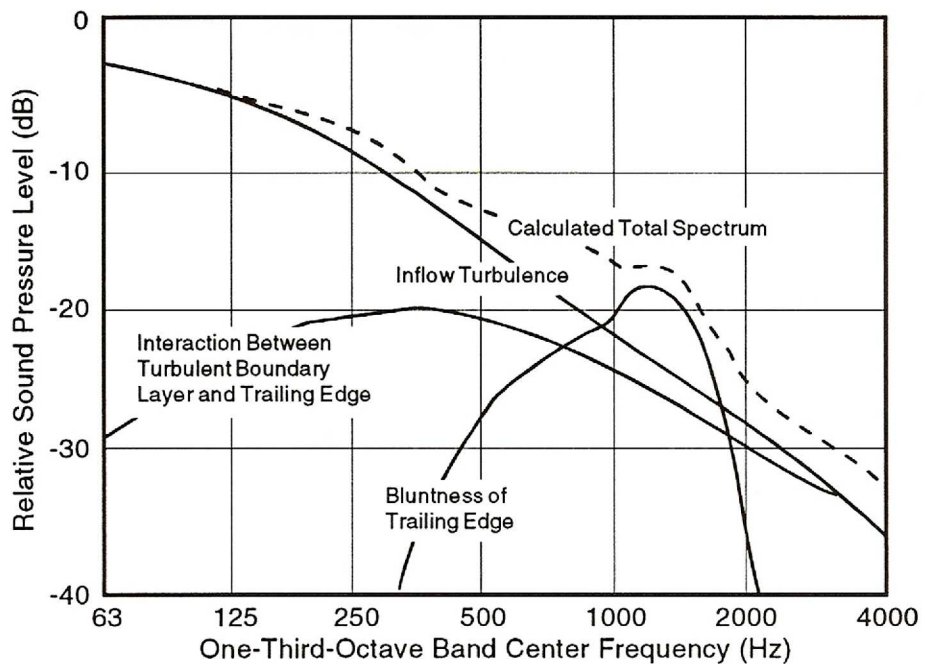


Figure 7-16. Relative contributions of broadband noise sources to the total noise spectrum calculated for a large-scale HAWT. [Grosveld 1985]

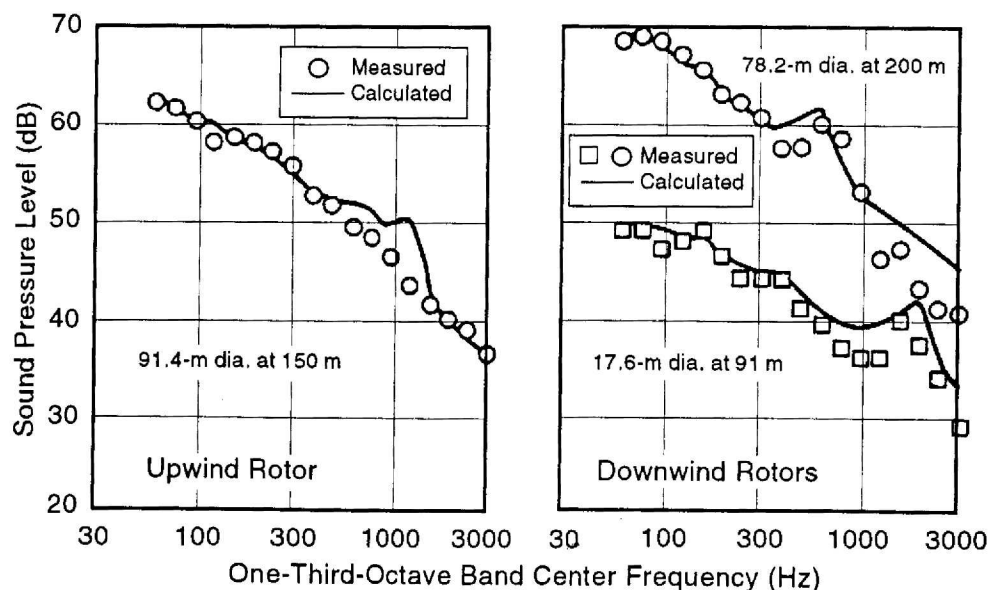


Figure 7-17. Measured and calculated broadband noise spectra downwind of various HAWTs. [Grosveld 1985]

An alternative broadband-noise prediction scheme is proposed in Glegg, Baxter, and Glendinning [1987] and includes noise from *unsteady lift, unsteady thickness, trailing edges, and separated flows*. Inflow turbulence at the rotor must be specified to predict unsteady lift and thickness noises. Using the turbulence data associated with the atmospheric boundary layer as input yielded poor agreement between calculated and measured noise levels. Thus, the authors hypothesized that there was an additional source of turbulence: that each blade ran into the tip vortex shed by the preceding blade. Note that Grosvenor [1985] also used atmospheric boundary layer turbulence but found that better agreement with acoustic measurements required an empirical turbulence model. The two approaches share the same theoretical background and therefore should give the same results.

## Noise Propagation

A knowledge of the manner in which sound propagates through the atmosphere is basic to the process of predicting the noise fields of single and multiple machines. Although much is known about sound propagation in the atmosphere, one of the least understood factors is the effect of the wind. Included here are brief discussions of the effects of distance from various types of sources, the effects of such atmospheric factors as absorption in air and refraction caused by sound speed gradients, and terrain effects.

### Distance Effects

#### *Point Sources*

When there is a nondirectional point source as well as closely-grouped, multiple point sources, *spherical spreading* may be assumed in the far radiation field. Circular wave fronts propagate in all directions from a point source, and the sound pressure levels decay at the rate of -6 dB per doubling of distance, in the absence of atmospheric effects. The latter decay rate is illustrated by the straight line in Figure 7-18. The dashed curves in the figure represent increased decay rates associated with *atmospheric absorption* at frequencies significant for wind turbine noise.

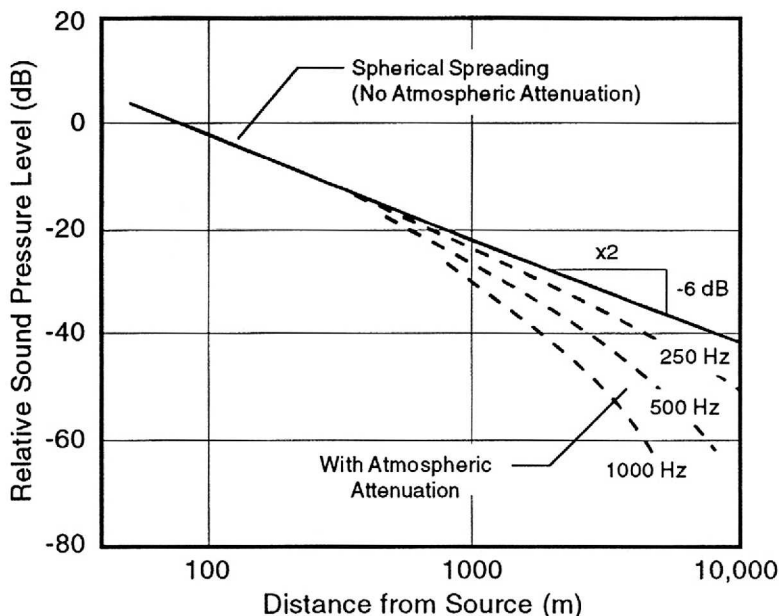


Figure 7-18. Decrease in the sound pressure levels of pure tones as a function of distance from a point source. [ANSI 1978]

### Line Sources

For an infinitely long line source, the decay rate is only -3 dB per doubling of distance, compared with the -6 dB per doubling of distance illustrated in Figure 7-18. Such a reduced decay rate is sometimes observed for sources such as trains and lines of vehicles on a busy road. Some arrays of multiple wind turbines in wind power stations may also behave acoustically like line sources.

### Atmospheric Factors

#### Absorption in Air

As sound propagates through the atmosphere, its energy is gradually converted to heat by a number of molecular processes such as shear viscosity, thermal conductivity, and molecular relaxation, and thus atmospheric absorption occurs. The curves in Figure 7-19 were plotted from ANSI values [1978] and show changes in atmospheric absorption as a function of frequency, at typical ambient temperatures and relative humidity levels. Atmospheric absorption is relatively low at low frequencies and increases rapidly as a function of frequency. Atmospheric absorption values for other temperature/humidity conditions can be obtained from the ANSI tables.

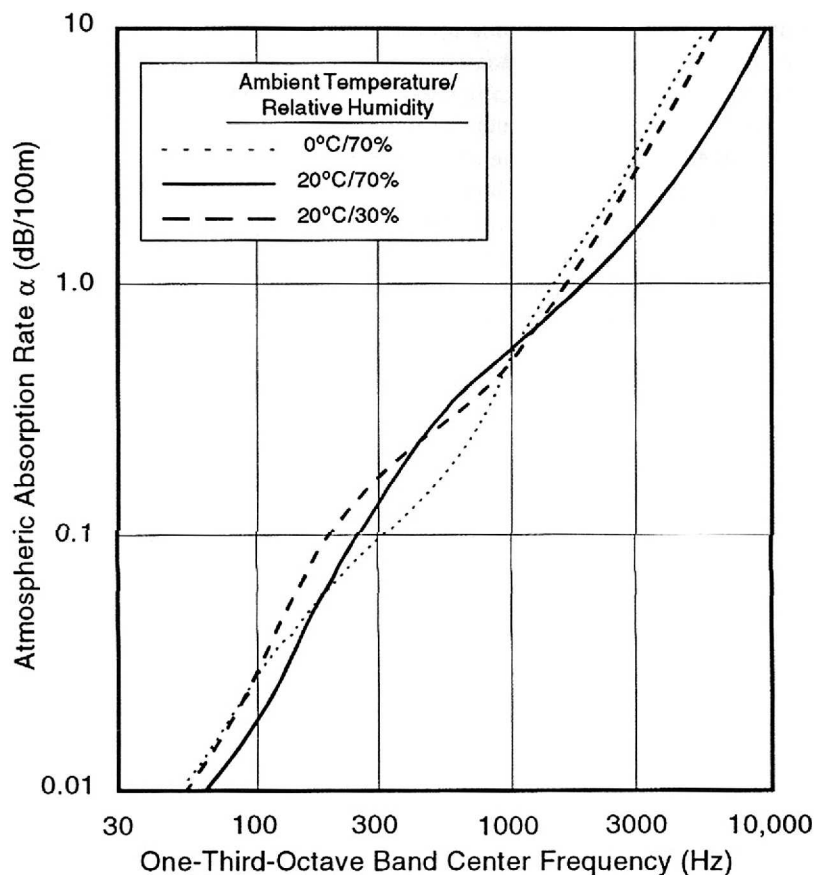


Figure 7-19. Standard rates of atmospheric absorption. [ANSI 1978]

#### Refraction Caused by Wind and Temperature Gradients

Refraction effects arising from the sound speed gradients caused by wind temperature can cause nonuniform propagation as a function of azimuth angle around a source. A simple illustration is shown in Figure 7-20 of *atmospheric refraction* (*i.e.*, bending) of sound rays, caused by a vertical wind-shear gradient over flat, homogeneous terrain around an elevated point source. Note that in the downwind direction the wind gradient causes the

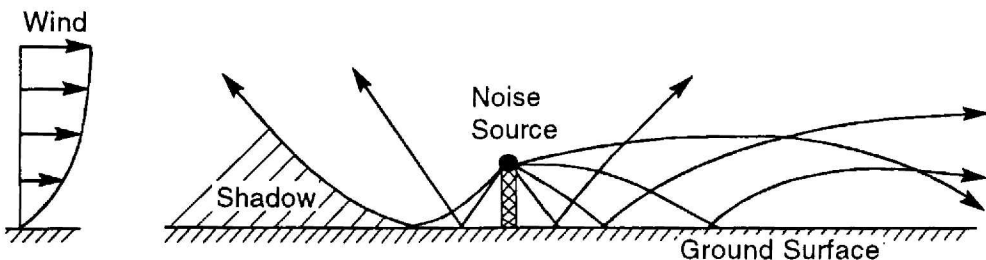


Figure 7-20. Effects of wind-induced refraction on acoustic rays radiating from an elevated point source. [Shepherd and Hubbard 1985]

sound rays to bend toward the ground, whereas in the upwind direction the rays curve upward away from the ground. For high-frequency acoustic emissions, this causes greatly increased attenuation in a *shadow zone* upwind of the source, but little effect downwind. The attenuation of a low-frequency noise, on the other hand, is reduced by refraction in the downwind direction, with little effect upwind.

The distance from the noise source to the edge of the shadow zone is related to the wind speed gradient and the elevation of the source. In a 10- to 15-m/s wind, for a source height from 40 to 120 m above flat, homogeneous terrain, the horizontal distance from the source to the shadow zone was calculated to be approximately five times the height of the source [Shepherd and Hubbard 1985].

Attenuation exceeding that predicted by spherical spreading and atmospheric absorption can be found in the shadow zone. This attenuation is frequency-dependent, and the lowest frequencies are the least attenuated. Figure 7-21 presents an empirical scheme for estimating attenuation in the shadow zone, based on information in Piercy, Embleton, and Sutherland [1977]; SAE [1966]; and Daigle, Embleton, and Piercy [1986]. The estimated extra attenuation is assumed to develop from zero to a maximum of  $A_E$  over a distance equal to twice that from the source to the edge of the shadow zone. The predicted decay in the sound pressure level from the source to the edge of the shadow zone is caused by atmospheric absorption [ANSI 1978] and spherical spreading. Within the shadow zone, extra attenuation should be added to these two effects, estimated according to Figure 7-21.

Note that vertical temperature gradients, which are also effective sound speed gradients, will normally be present. These will add to or subtract from the effects of wind that are illustrated in Figure 7-20. Effects of the wind gradient will generally dominate over those of temperature gradients in the propagation of noise from wind power stations.

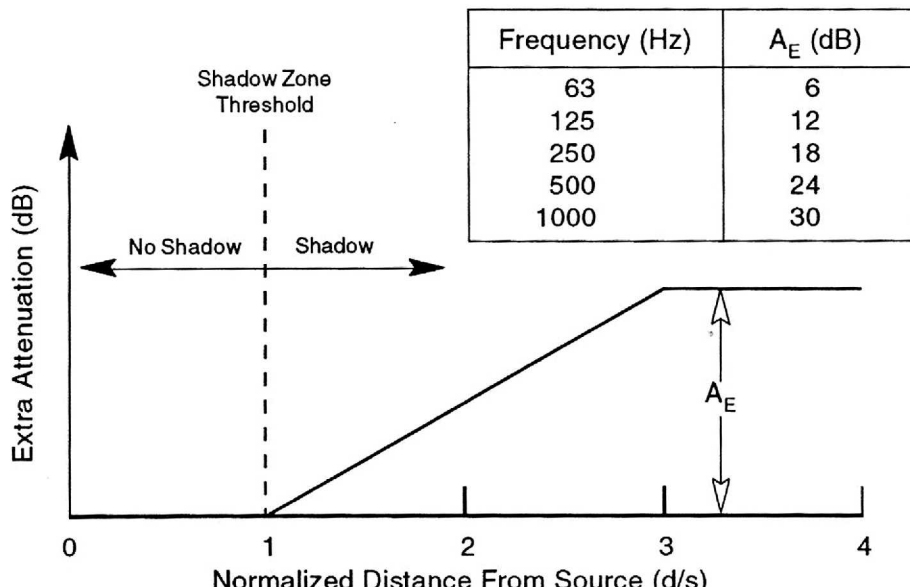
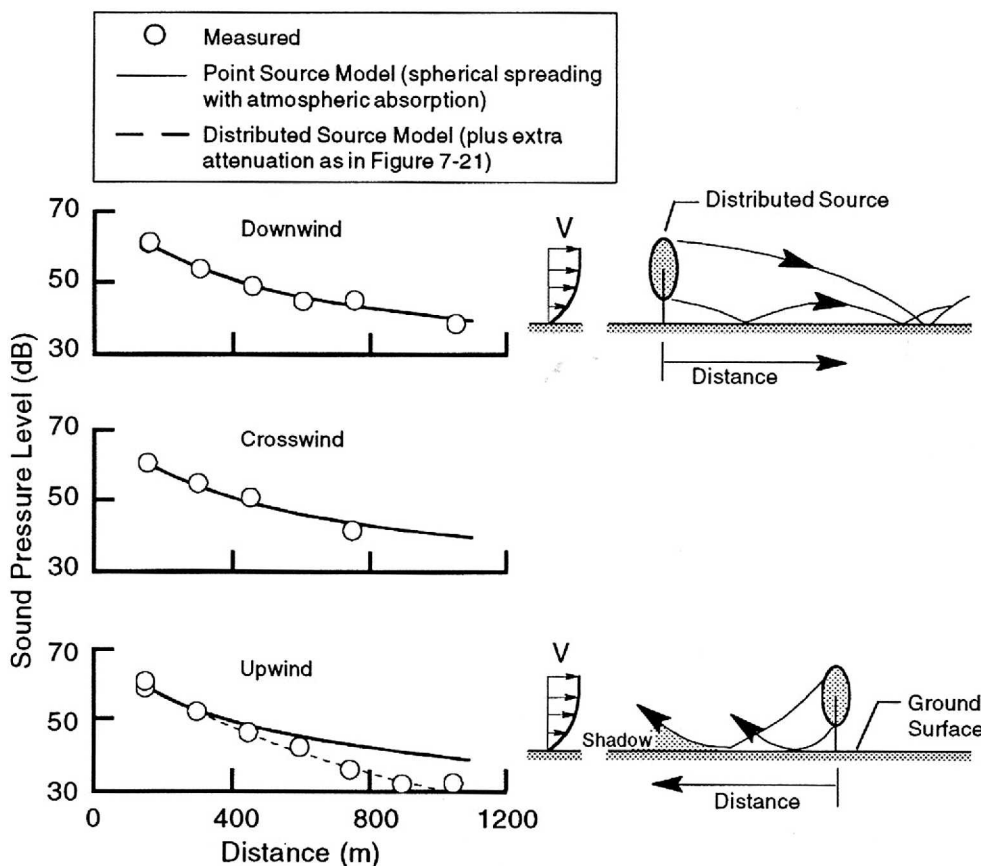


Figure 7-21. Empirical model for estimating the extra attenuation of noise in the shadow zone upwind of an elevated point source. ( $s = 5h$ ,  $40 \leq h \leq 120$  m, where  $h$  = source elevation) [Shepherd and Hubbard 1985]

*Distributed Source Effects*

Because of their large rotor diameters, some wind turbines exhibit distributed source effects relatively close to the machines. Only when listeners are at distances from a turbine that are large in relation to its rotor diameter does the rotor behave acoustically as a point source. As indicated in Figure 7-22, distributed source effects are particularly important in the upwind direction. In this figure, sound pressure levels in the 630-Hz, one-third-octave band are presented as a function of distance in the downwind, upwind, and crosswind directions. In the downwind and crosswind directions, the measured data agree well with the solid curves representing spherical spreading and atmospheric absorption. In the upwind direction, however, the measured data fall below the solid curve, which indicates the presence of a shadow zone.

An improvement in predicting upwind sound pressure levels is obtained when the noise is modeled as being distributed over the entire rotor disk. Each part of the disk is then considered to be a point source, and attenuation is estimated by means of the empirical model shown in Figure 7-21. The resulting predictions are shown as the dashed curve of Figure 7-22 and are in good agreement with the sound measurements upwind of the turbine. In the downwind and crosswind directions, point-source and distributed-source models result in identical calculations of sound pressure levels.



**Figure 7-22. Measured and calculated sound pressure levels in three directions from a large-scale HAWT. (one-third-octave band = 630 Hz, rotor diameter = 78.2 m) [Shepherd and Hubbard 1985]**

Figure 7-23 illustrates the special case of propagation of low-frequency rotational-harmonics when the atmospheric absorption and extra attenuation in the shadow zone are very small. Measured sound pressure levels are shown as a function of distance for both the upwind and downwind directions. For comparisons, the curves representing decay rates of -6 dB and -3 dB per doubling of distances are also included. Note that in the upwind case the sound pressure levels tend to follow a decay rate of -6 dB per doubling of distance, which is equal to the rate of spherical spreading. No extra attenuation from a shadow zone was measured.

In the downwind direction, the sound pressure levels tend to follow a decay rate of -3 dB per doubling of distance, similar to that for cylindrical spreading. This reduced decay rate in the downwind direction at very low frequencies is believed to result from atmospheric refraction which introduces a channeling sound path in the lower portions of the earth's boundary layer [Willshire and Zorumski 1987, Thomson 1982, Hawkins 1987].

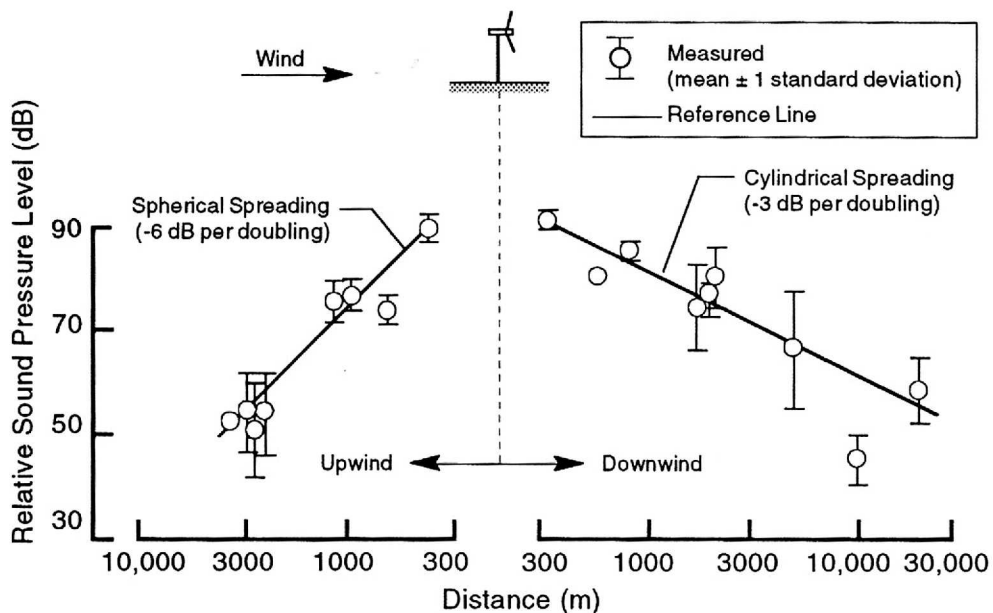


**Figure 7-23. Measured effect of wind on the propagation of low-frequency rotational harmonic noise from a large-scale HAWT.** (Harmonics with frequencies from 8 to 16 Hz, rotor diameter = 78.2 m) [Willshire and Zorumski 1987]

## Terrain Effects

Terrain effects include ground absorption, reflection, and diffraction. Furthermore, terrain features may cause complex wind gradients, which can dominate noise propagation to large distances [Kelley *et al.* 1985, Thompson 1982]. Wind turbines are generally located in areas devoid of trees and other large vegetation. Instead, ground cover usually consists of grass, sagebrush, plants, and low shrubs, which are minor impediments to noise propagation except at very high frequencies. At frequencies below about 1,000 Hz, the ground attenuation is essentially zero.

Methods are available for calculating the attenuations provided by natural barriers such as rolling terrain, which may interrupt the line of sight between the source and the receiver [Piercy and Embleton 1979]. However, very little definitive information is available regarding the effectiveness of natural barriers in the presence of strong, vertical wind gradients. Piercy and Embleton [1970] postulate that the effectiveness of natural barriers in attenuating noise is not reduced under conditions of upward-curving ray paths (as would apply in the upwind direction) or under normal temperature-lapse conditions. However, under conditions of downward-curving ray paths, as in downwind propagation or during temperature inversions (which are common at night), the barrier attenuations may be reduced significantly, particularly at large distances.

## Predicting Noise from Multiple Wind Turbines

Methods are needed to predict noise from wind power stations made up of large numbers of machines, as well as for a variety of configurations and operating conditions. This section reviews the physical factors involved in making such predictions and presents the results of calculations that illustrate the sensitivity of radiated noise to various geometric and propagation parameters. A number of valid, pertinent, simplifying assumptions are presented. A logarithmic wind gradient is assumed, with a wind speed of 9 m/s at hub height. Flat, homogeneous terrain, devoid of large vegetation, is also assumed. Noises from multiple wind turbines are assumed to add together incoherently, that is, in random phase.

## Noise Sources and Propagation

### Reference Spectrum for a Single Wind Turbine

The most basic information needed to predict noise from a wind power station is the noise output of a single turbine. Its noise spectrum can be predicted from knowledge of the geometry and operating conditions of the machine [Viterna 1981; Glegg, Baxter, and Glendinning 1987; Grosveld 1985], or its spectrum can be measured at a reference distance. Figures 7-9 and 7-10 are examples of spectral data for HAWTs. The solid line shown in Figure 7-10 is a hypothetical spectrum used in subsequent example calculations to represent a HAWT with a 15-m rotor diameter and a rated power of approximately 100 kW. The example spectrum has a decrease of 10 dB per decade in sound pressure level with increasing frequency. This spectral shape is generally representative of the aerodynamic noise radiated by wind turbines. However, predictions for a specific wind power station should be based, if possible, on data for the particular types of turbines in the station.

### Directivity of the Source

Measurement of aerodynamic noise for a number of large HAWTs [e.g., Kelley *et al.* 1985, Hubbard and Shepherd 1982] indicate that the source directivity depends on specific noise-generating mechanisms. For broadband noise sources, such as inflow turbulence and interactions between the blade boundary layer and the blade trailing edge, sound pressure level contours are approximately circular. Lower-frequency, impulsive noise, which results when the blades interact with the tower or central column wake, radiates most strongly in the upwind and downwind directions. Furthermore, while there is one prevailing wind direction at most wind turbine sites, it is not uncommon for the prevailing wind vector to

vary  $\pm 45$  deg in azimuth angle during normal operations. Therefore, one of the simplifying assumptions made in the calculations that follow is that each individual machine behaves like an *omnidirectional source*.

#### Considerations for Frequency Weighting

*A-weighted* sound pressure levels, expressed in dB(A), are in widespread use for evaluating the effects of noise on communities [Pearsons and Bennett 1974]. This particular weighting emphasizes the higher frequencies and de-emphasizes the lower frequencies, according to the sensitivity of the human ear. Figure 7-24 shows the results of applying this descriptor. The solid line is the assumed single-turbine reference spectrum, at a distance of 30 m from the machine, and the upper dashed curve is the equivalent A-weighted spectrum at the same distance. As distances increase, atmospheric absorption causes the levels of the higher-frequency components to decay faster than those of the lower frequencies (see Figure 7-19).

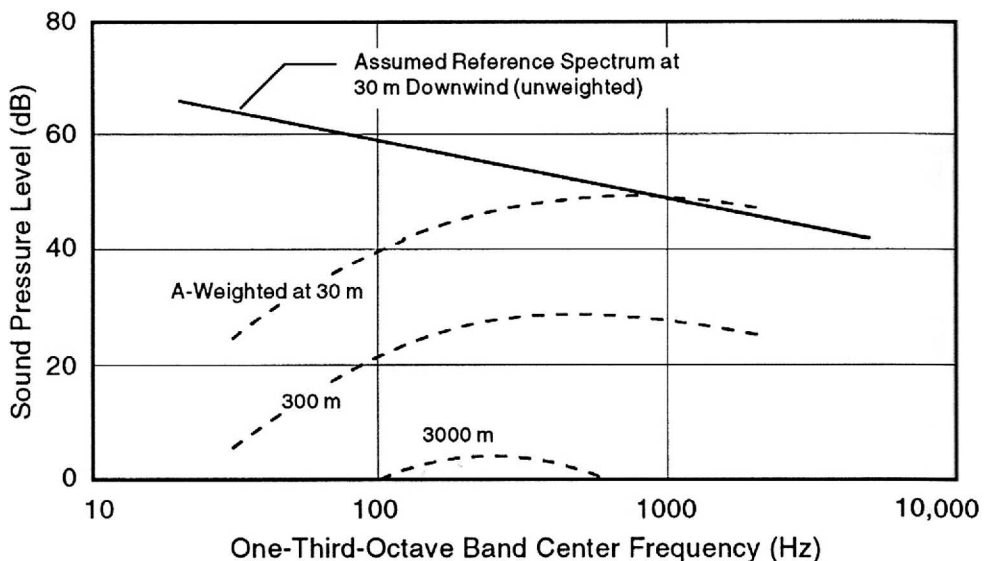


**Figure 7-24. Reference and A-weighted noise spectra from a 15-m-diameter HAWT with a rated power of 100 kW.** Assumed for example calculations of noise from a wind power station

The result of the combination of A-weighting and atmospheric absorption is that the midrange frequencies (100 to 1000 Hz) tend to dominate the audible spectrum at long distances. Frequencies higher than 1000 Hz will generally not be important considerations at long distances because of the effects of atmospheric absorption. Frequency components below about 100 Hz may not be significant in terms of audible noise, but they can be significant in terms of such indirect effects as noise-induced building vibrations.

#### Representative Wind Power Station

The basic geometric arrangement of wind turbines shown in Figure 7-25 is assumed to represent an example wind power station. The station consists of four rows, with 31 100-kW, 15 m-diameter turbines per row. The spacing between turbines is 30 m, the row length is 900 m, and the spacing between rows is 200 m. This basic four-row configura-

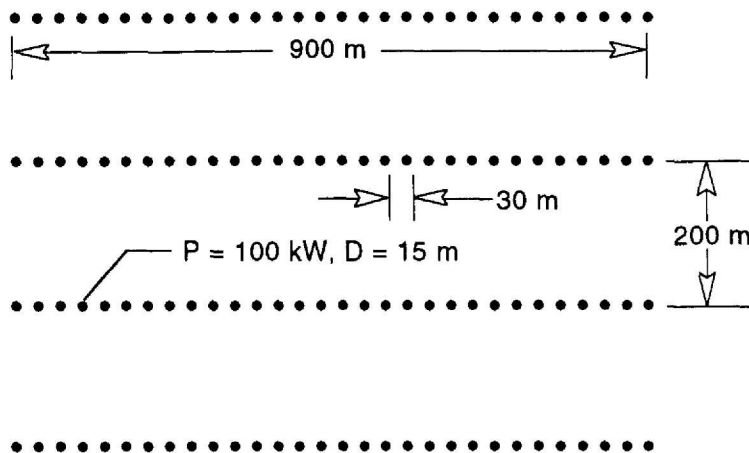


**Figure 7-25.** Layout of 124 wind turbines in a representative wind power station. [Shepherd and Hubbard 1986]

tion can be perturbed to investigate the effects of such variables as the number of rows, row spacing, turbine spacing, row length, and turbine power rating.

#### Absorption and Refraction

The example calculations that follow assume an ambient temperature of 20° C and a relative humidity of 70%. From the data in Figure 7-19, assumed values of atmospheric absorption of 0, 0.10, 0.27, and 0.54 dB per 100 m then correspond roughly to one-third-octave band center frequencies of 50, 250, 500 and 1,000 Hz, respectively. These frequencies were chosen because they encompass the range of frequencies considered important in evaluating the perception of wind turbine noise in adjacent communities [Shepherd and Hubbard 1986].

#### Calculation Methods

The method presented here for calculating the sound pressure level from incoherent addition is a sum of the random-phase multiple noise sources at any arbitrary receiver distance. This method assumes that each source radiates equally in all directions, and attenuation caused by atmospheric absorption is included. Propagation is over flat, homogeneous terrain, and there is a logarithmic wind-speed gradient. The method has no limitations on the number of wind turbines or their geometric arrangement.

The required input is a reference sound-pressure-level spectrum,  $L_0(f)$ , either narrow-band or one-third-octave band, for a single wind turbine. This spectrum can be either measured or predicted, and should represent the radiated noise at a reference turbine-to-receiver distance of approximately 2.5 times the rotor diameter. The sound pressure level

1 received from any individual wind turbine in the array in a given frequency band can then be  
 2 calculated with the following equation:  
 3

$$L_n(f_i) = L_0(f_i) - 20 \log_{10}(d_n/d_0) - \alpha(d_n/d_0)/100 \quad (7-8)$$

4 where  
 5  
 6

- 7      $L_n(f_i)$  = sound pressure level in the  $i$ th frequency band from the  $n$ th turbine (dB)  
 8          $n$  = wind turbine index = 1,2,...,N  
 9          $N$  = number of wind turbines in the power station  
 10         $f_i$  = center frequency of the  $i$ th band (Hz)  
 11         $L_0(f_i)$  = sound pressure level from the reference wind turbine in the  $i$ th frequency  
 12        band at the reference distance (dB)  
 13         $d_n$  = distance from the  $n$ th turbine to the receiver (m)  
 14         $d_0$  = reference turbine-to-receiver distance (m)  
 15         $\alpha$  = atmospheric absorption rate (dB per 100 m)

16 The total sound pressure level in the  $i$ th frequency band, from all wind turbines in the array,  
 17 is then calculated as follows:  
 18

$$SPL_{total}(f_i) = 10 \log_{10} \sum_n 10^{L_n(f_i)/10} \quad (7-9)$$

20 This procedure is repeated for all frequency bands to provide a predicted spectrum of sound  
 21 pressure levels at the receiver location. Noise measures such as the A-weighted sound  
 22 pressure level may also be calculated by adding the A-weighting corrections at each  
 23 frequency to the values of  $L_n(f_i)$  or  $SPL_{total}(f_i)$  in Equations 7-8 and 7-9. If the sources are  
 24 arranged in rows, the required computations can be reduced by using the simplified proce-  
 25 dures of Shepherd and Hubbard [1986].  
 26

### 33 Examples of Calculated Noise from Wind Power Stations

34 A series of parametric calculations of unweighted sound pressure levels has been per-  
 35 formed based on the array of Figure 7-25 and systematic variations of that array [Shep-  
 36 herd and Hubbard 1986]. The receiver is assumed to be on a line of symmetry either in the  
 37 downwind, upwind, or crosswind direction.  
 38

#### 40 Effect of Distance from a Single Row

41 Figure 7-26 shows calculated sound pressure levels from one row of the example wind  
 42 power station, as a function of downwind distance for various rates of atmospheric absorp-  
 43 tion. Also shown are reference decay rates of -3 dB and -6 dB per doubling of distance.  
 44 For an atmospheric absorption rate of zero, the decay rate is always less than that for a  
 45 single point source (Figure 7-18). At intermediate distances, the row of turbines acts as a  
 46 line source, for which the theoretical decay rate is -3 dB per doubling of distance (or -10  
 47 dB per decade of distance). Only at distances greater than one row length (900 m in this  
 48 case) does the decay rate approach the single-point-source value of -6 dB per doubling of  
 49 distance (-20 dB per decade). Decay rates increase as the absorption coefficient increases.  
 50

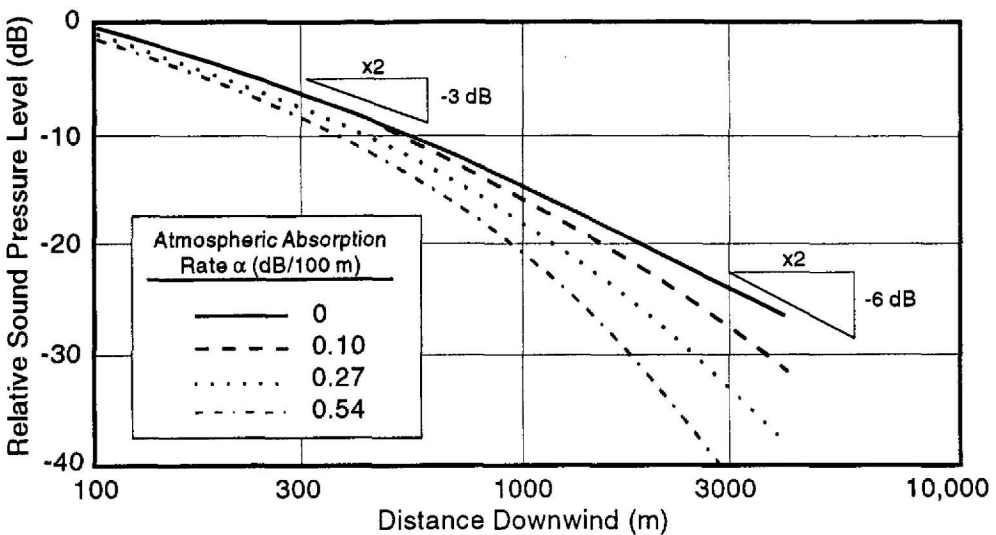


**Figure 7-26.** Calculated noise propagation downwind of a single row of wind turbines in the example array for four atmospheric absorption rates. [Shepherd and Hubbard 1986]

#### Effect of Multiple Rows

Figure 7-27 presents the results of sound-pressure-level calculations that were made for one, two, four, and eight rows of wind turbines; this illustrates the effects of progressively doubling the number of machines for a constant turbine spacing. At zero atmospheric absorption, and at receiver distances that are large relative to the array dimensions, a doubling of the number of rows results in an increase of 3 dB in the sound pressure level. This simply reflects a doubling of acoustic power. At shorter distances, the closest machines dominate and the additional rows result in only small increments in the sound

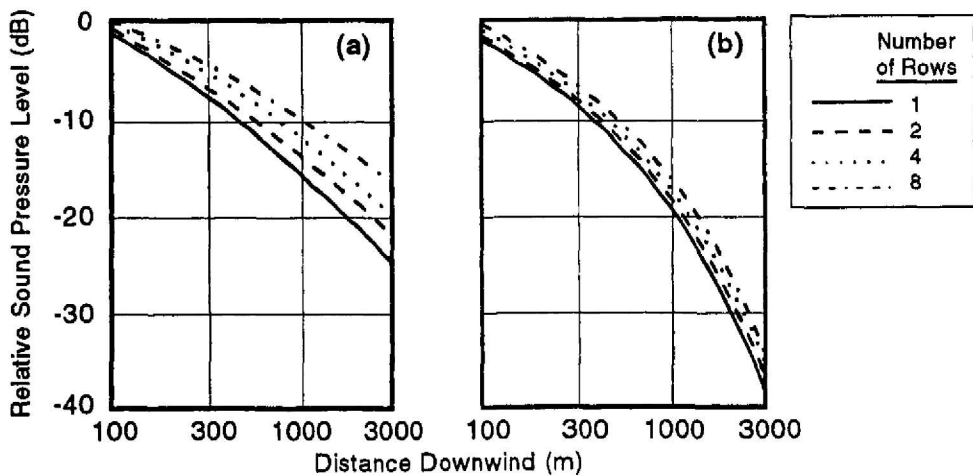


**Figure 7-27.** Calculated noise propagation downwind of various numbers of rows of wind turbines in the example array. [Shepherd and Hubbard 1986] (a) Without atmospheric absorption. (b) Absorption coefficient  $\alpha = 0.54$  dB/100 m

pressure level. For nonzero atmospheric absorption, the effect of additional rows is less significant at all receiver distances. Doubling the number of rows results in an increase in the sound pressure level of less than 3 dB.

Figure 7-28 shows similar data for two different row lengths. For these comparisons, the turbine spacing is constant and the row lengths are doubled by doubling the number of machines per row. When the receiver is at shorter distances, the predicted sound pressure levels are equal because of the equal turbine spacing. At longer distances, the levels for the double-length row are higher by 3 dB because the acoustic power per row is doubled.

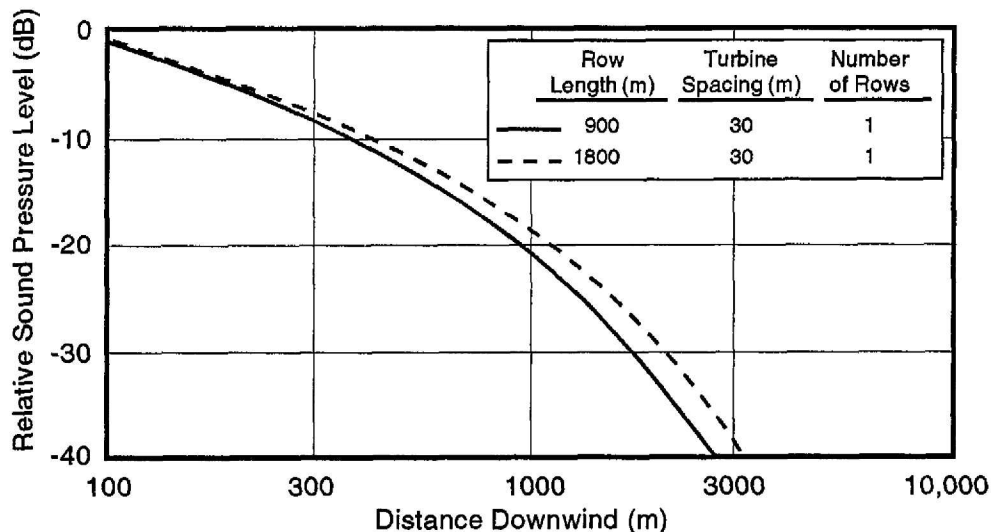


**Figure 7-28. Calculated noise propagation downwind of wind turbines in rows of two different lengths. ( $\alpha = 0.54 \text{ dB}/100 \text{ m}$ ) [Shepherd and Hubbard 1986]**

Computations were also made [Shepherd and Hubbard 1986] for a configuration similar to that of Figure 7-25, except that the row spacing was reduced from 200 m to 100 m. At all distances to the receiver, the computed sound pressure levels were higher for this more compact array.

#### *Effect of Turbine Rated Power*

Shepherd and Hubbard [1986] calculated the effect of the turbine's rated power on noise emissions by increasing the power of each turbine and the total station power. The turbine and row spacings were adjusted from those of Figure 7-25 to more appropriate values for larger machines (four times the rated power). Sound pressure levels from rows of 16 400-kW wind turbines were compared with levels from the same number of rows of 31 100-kW machines. This approximately doubled the rated power of the station. The reference spectrum for the larger turbines was assumed to have the same shape as that of the smaller turbines (Figure 7-10), although the levels were all 6 dB higher. This implies four times the acoustic power for four times the rated power. The computed sound pressure levels are 3 dB higher for the array of larger turbines because the acoustic power is doubled for each row of the array. Different results would be obtained if the reference spectra of the two sizes of turbines had different shapes.

*Directivity Considerations for a Wind Power Station*

Although individual turbines have been treated as if they radiate sound equally in all directions, an array of such sources may not have uniform directivity characteristics. Figure 7-29 compares the predicted sound pressure levels for two array configurations as received from two different directions. Calculations are presented for a receiver located downwind on the line of symmetry perpendicular to the rows and for a receiver located crosswind on the line of symmetry parallel to the rows. For the case of one row of turbines, the crosswind sound pressure level is predicted to be about 5 dB lower than the downwind level near the turbines, and only about 2 dB lower in the far field. For an array with eight rows, the crosswind sound pressure level is only 3 dB lower near the turbines, and there is little directivity once the receiver distance exceeds 300 m. Downwind levels are higher close to the eight-row array, because the turbine spacing in the row is less than the row spacing.

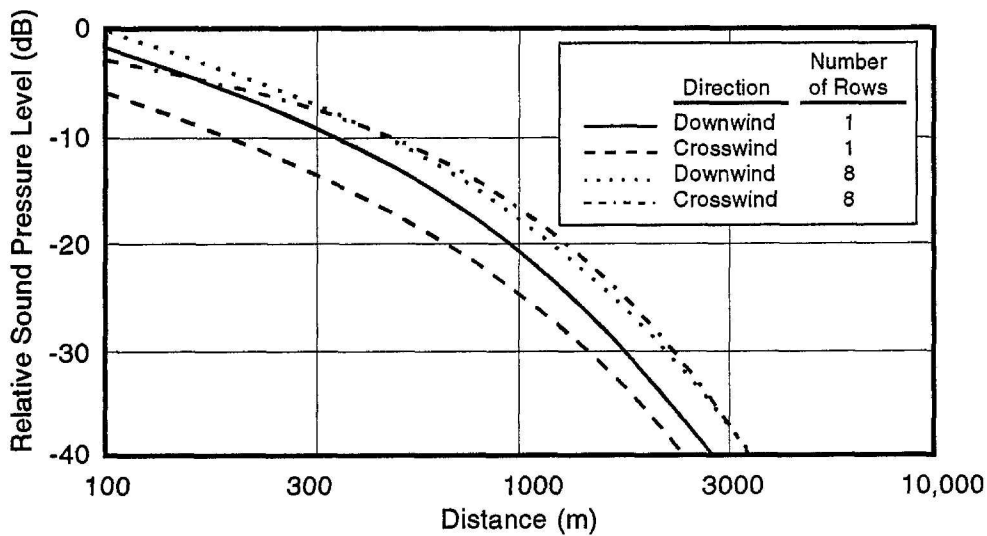


**Figure 7-29. Calculated noise propagation downwind and crosswind of single and multiple rows of wind turbines in the representative wind power station. ( $\alpha = 0.54$  dB/100 m)[Shepherd and Hubbard 1986]**

Estimates of complete contours of sound pressure level around a wind power station are shown in Figure 7-30. The array geometry in this case consists of five rows of 31 machines each, spaced as shown in Figure 7-25. This gives an approximately square array. Figure 7-30 shows predicted contours for sound pressure levels of 40, 50, and 60 dB for an atmospheric absorption rate of 0.54 dB/100 m (which corresponds to a frequency of 1000 Hz, at 20°C and 70% relative humidity). Assuming a hub-height wind speed of 9 m/s, the distances to contours in the upwind direction are greatly reduced. These upwind contours are derived from computed distances to the acoustic shadow zone and the extra attenuation that occurs within this zone (see Figure 7-21).

An acoustic shadow zone forming upwind of the array results in greatly reduced distances to particular noise level contours (*i.e.*, greatly reduced noise propagation) for all frequencies above about 60 Hz. The dashed curve in Figure 7-30 shows the location of the 40-dB contour in the absence of a shadow zone.

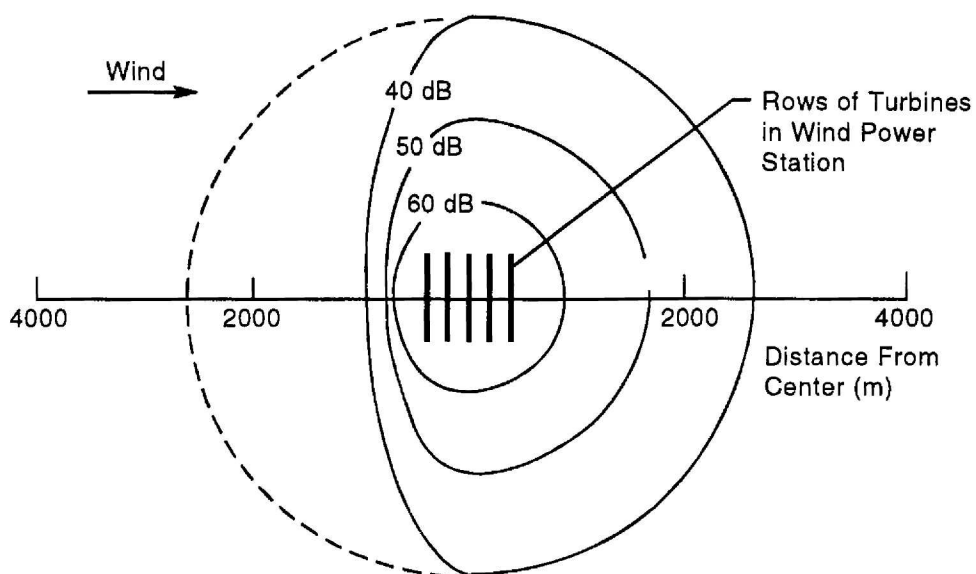


Figure 7-30. Calculated contours of sound pressure level around a five-row example array for the one-third-octave band at 1000 Hz. ( $\alpha = 0.54 \text{ dB}/100 \text{ m}$ ) [Shepherd and Hubbard 1986]

#### A-Weighted Composite Spectra

Figure 7-31 illustrates the effects of A-weighting the composite sound spectrum from the representative wind power station. Predicted sound spectra for the array are compared with equivalent spectra for a single machine (Figure 7-24). At large distances, the midrange frequencies dominate the A-weighted spectrum for both the single turbine and the array.

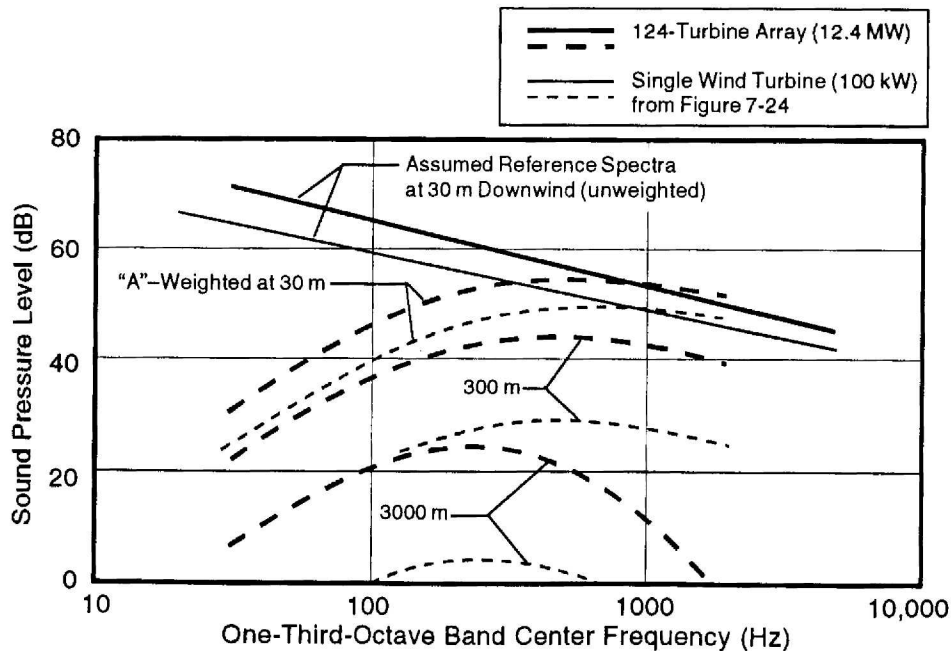
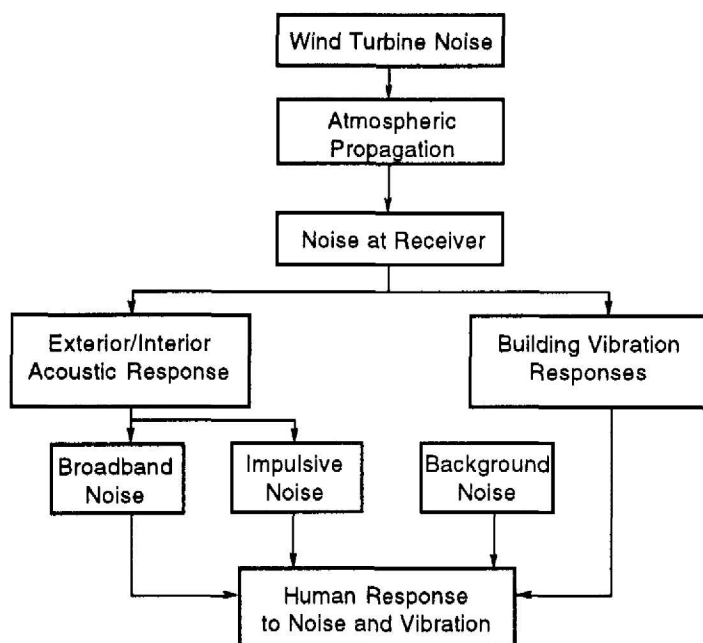


Figure 7-31. Reference and A-weighted noise spectra for the representative 124-turbine wind power station and for a single wind turbine [Shepherd and Hubbard 1986]

## Receiver Response

Evaluating the effect of receivers' exposure to noise at various locations involves determining people's responses to direct acoustic radiation as well as the acoustic and vibrational environments inside buildings. The factors involved in such an evaluation are diagrammed in Figure 7-32 and are explained in detail in Stephens *et al.* [1982]. Noise radiated by the wind turbine is propagated through the atmosphere to a receiver (a person or a building), and the characteristics of that receiver then determine the acoustic and vibration effects of the noise. The broadband and impulsive components of the acoustic response are treated separately, and either may be significant. Background noise and building vibrations must also be considered in evaluating people's responses to wind turbine noise.



**Figure 7-32. Factors and interactions to be considered in evaluating human response to wind turbine noise [Stephens *et al.* 1982]**

If wind turbine noise levels are below the corresponding background noise levels, they will generally not be perceived; therefore, no adverse human response is expected. When any noise level exceeds the *threshold of perception*, however, there is the potential for community response, as indicated in Table 7-1 [ISO 1971]. The data in this table were derived from responses to noise sources other than wind turbines. Because there has been little experience to date with community responses to wind turbines, the applicability of Table 7-1 is tentative. The substantial variations in background noise in terms of time-of-day and location are complicating factors.

Perception thresholds for acoustic noise and structural vibrations have been derived separately. There are no known threshold criteria for combined effects, except in terms of the quality of the ride in transportation vehicles [Stephens 1979].

Table 7.1. Estimated Community Response to Noise (ISO 1971)

Amount by which received noise exceeds threshold level (dB)	Estimated community response	
	Category	Description
0	None	No observed reaction
5	Little	Sporadic complaints
10	Medium	Widespread complaints
15	Strong	Threats of community action
20	Very Strong	Vigorous community action

## Perception of Noise Outside Buildings

Evaluating people's responses to wind turbine noise outside buildings involves the physical characteristics of the noise of the machines, the pertinent atmospheric phenomena, and the ambient or outdoor background noise at the receiver's location. Both broadband and narrow-band noise components must be considered if they are present in the noise spectrum.

In Figure 7-33, a one-third-octave band spectrum of broadband wind turbine noise is compared with a one-third-octave band spectrum of the typical background noise in a residential neighborhood. In this case, the background noise is a combination of noises from numerous distant sources, with no dominant specific source. Wind effects are also absent. Note that the turbine noise levels are generally lower than the background noise levels, except at 1000 Hz, where they are about equal. In the laboratory, human subjects exposed to the spectra of Figure 7-33 can just perceive the wind turbine noise. High-frequency wind turbine noise is generally not perceived in laboratory tests when the turbine's one-third-octave band levels are below the corresponding levels of background noise (which, in this case, had small temporal fluctuations).

The same general findings apply to the perception of low-frequency impulsive noise. A series of laboratory tests [Stephens *et al.* 1982; Shepherd 1985] were conducted to determine the detection thresholds of impulsive wind turbine noises in the presence of ambient noise with a spectral shape similar to that in Figure 7-33. In contrast to the relatively simple detection model for higher-frequency noises, understanding the perception of low-frequency impulsive noise requires that a full account be taken of the blade passage frequency of the wind turbine, the ambient noise spectrum, and the absolute hearing threshold. The latter is important because the human ear is relatively insensitive to the low frequencies that characterize impulsive wind turbine noise.

In addition to laboratory tests with sample spectra, field tests can be used to determine thresholds of perception around wind turbines, including directivity effects. For example, aural (hearing) detectability contours were determined for two large-scale HAWTs surrounded by flat terrain. The results are shown in Figure 7-34.

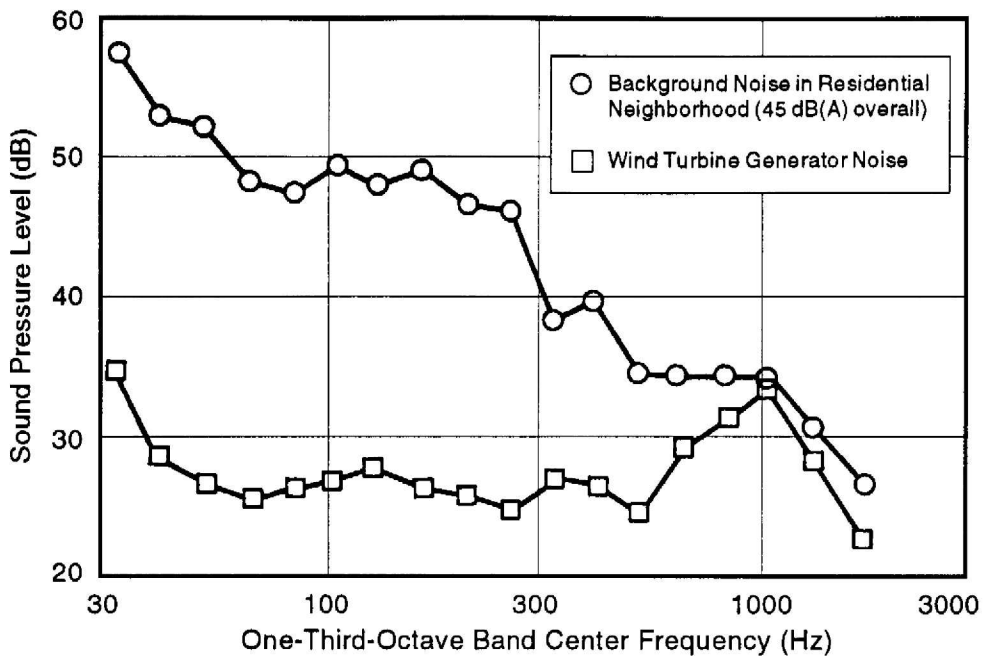


Figure 7-33. Example broadband noise spectrum at the perception threshold in the presence of the given background noise spectrum. [Stephens *et al.* 1982]

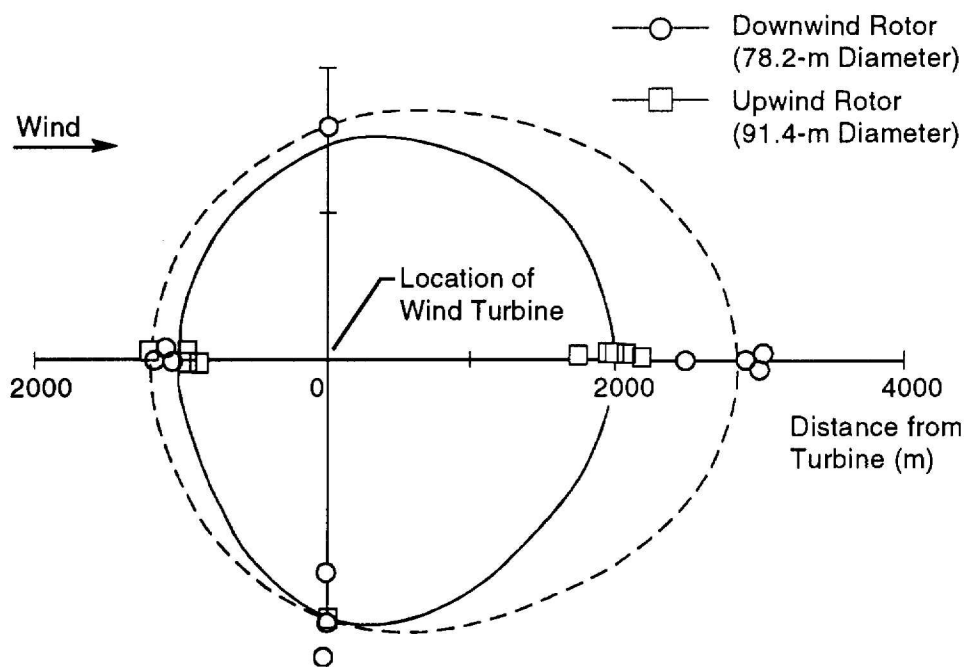


Figure 7-34. Perception thresholds for large-scale HAWTs with downwind and upwind rotors.

In Figure 7-34, each data point represents observations by one or two people and defines the distance at which the wind turbine noise is heard intermittently. The two aural curves in the figure are then estimated from these observations and from a limited number of sound pressure measurements. Both curves are foreshortened in the upwind direction and elongated in the downwind direction. With one exception, broadband noise was the dominant component perceived for both HAWTs. The exceptional case is that of noise downwind of the downwind-rotor machine, for which low-frequency impulses are the dominant component. This accounts for its longer downwind detection distance as compared with that of the upwind-rotor turbine.

## Background Noise

Because background noise is an important factor in determining people's responses to wind turbine noise, it must be carefully accounted for by site measurements without the wind turbines operating, and preferably prior to their construction. Sources of background noise are the wind itself; its interaction with structures, trees, and vegetation; human activities; and, to a lesser extent, birds and animals. Natural wind noises are particularly important because they can mask wind turbine noise, as a result of the fact that their broadband spectra are similar to those of wind turbines. Measuring background noise, at the same locations and with the same techniques used for measuring wind turbine noise, is an integral part of assessing receiver response.

## Noise Exposure Inside Buildings

People who are exposed to wind turbine noise inside a building experience a much different acoustic environment than do those outside. The noise transmitted into the building is affected by the mass and stiffness characteristics of the structure, the dynamic response of structural elements, and the dimensions and layouts of rooms. People may actually be more disturbed by the noise inside their homes than they would be outside [Kelley *et al.* 1985]. Indoor background noise is also a significant factor.

Data showing the reductions in outdoor noise provided by typical houses are given in Figure 7-35 as a function of frequency. The hatched area shows experimental results obtained from a number of sources [Stephens *et al.* 1983]. The noise reduction values of the ordinate are the differences between indoor and outdoor levels. The most obvious conclusion here is that noise reductions are larger at higher frequencies. This implies that a spectrum measured inside a house will have relatively less high-frequency content than that measured outside. These data are derived from octave-band measurements but are generally not sensitive to frequency bandwidth.

Very few data are available on outdoor-to-indoor noise reduction at the lowest frequencies (*i.e.*, below 50 Hz). In this range, wavelengths are comparable to the dimensions of rooms, and there is no longer a diffuse sound field on the inside of the building. Other complicating factors are low-frequency building resonances and air leaks. The inside distribution of sound pressure can be nonuniform because of structure-borne sound, standing wave patterns, and cavity resonances in rooms, closets, and hallways.

Data relating to the noise-induced vibration responses of houses are summarized in Figure 7-36, in which RMS acceleration levels are plotted as a function of external sound pressure level. The trend lines for windows, walls, and floors are averaged from a large number of test measurements of aircraft and helicopter noises, sonic booms, and wind turbine noise.

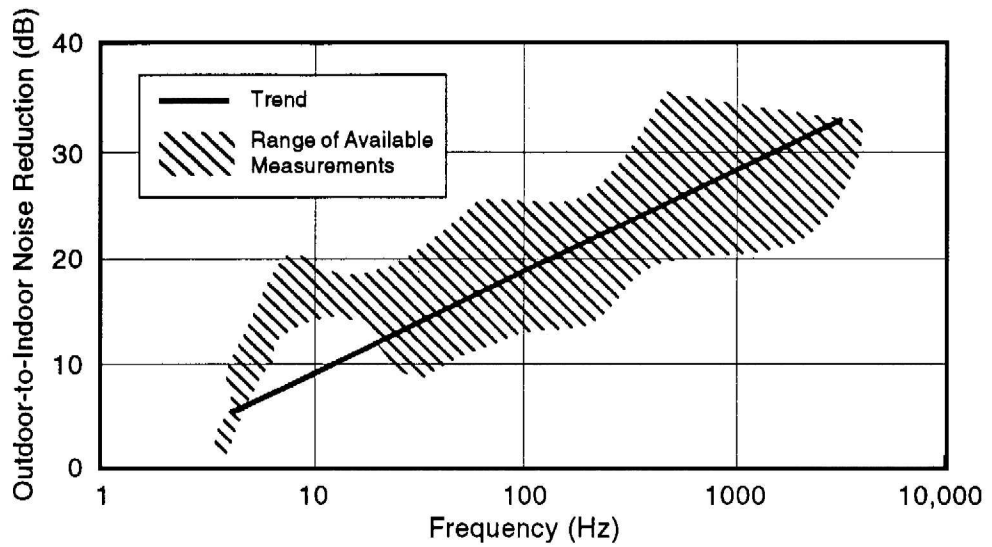


Figure 7-35. Outdoor-to-indoor noise reduction in a typical house with closed windows. [Stephens *et al.* 1982]

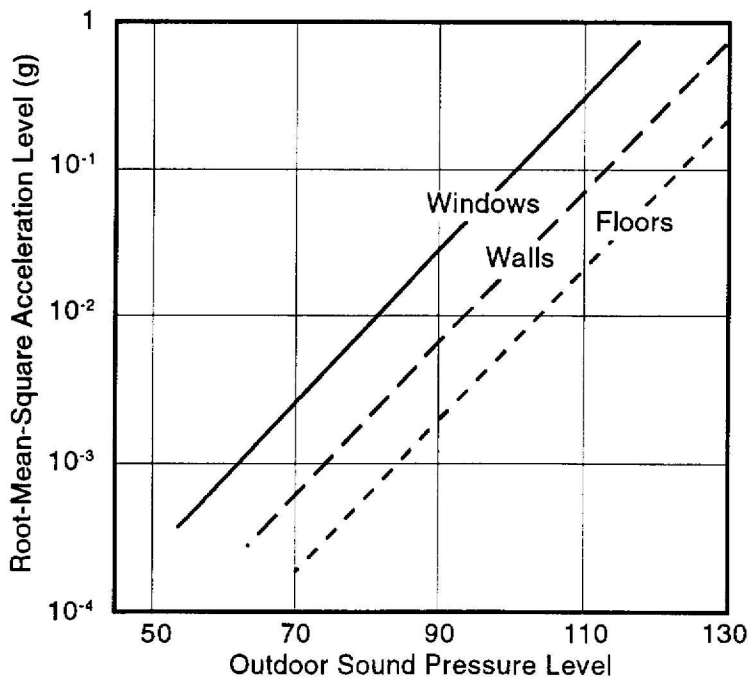


Figure 7-36. The noise-induced acceleration of the typical structural elements of a house, as a function of outdoor sound pressure level. [Stephens *et al.* 1982]

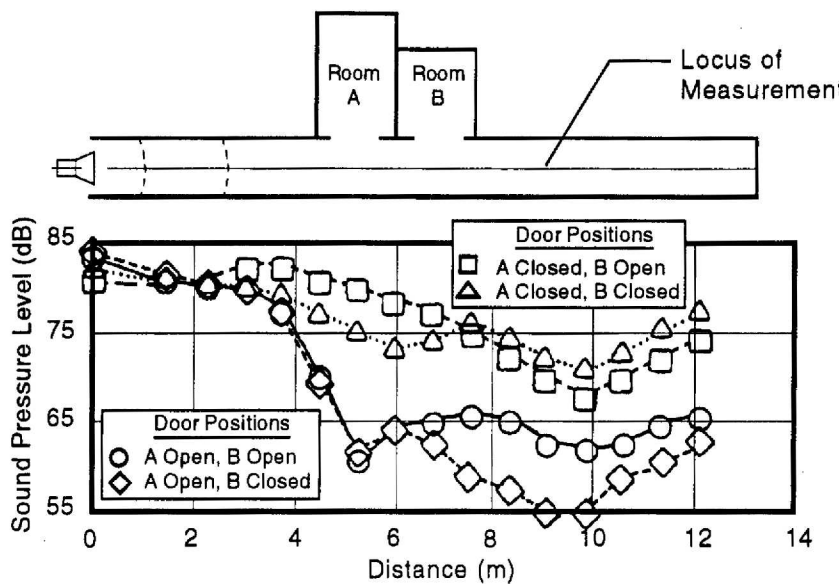


Figure 7-37. Sound-pressure-level gradients in a hallway excited by a pure-tone (21 Hz), constant-power loudspeaker. [Hubbard and Shepherd 1986]

#### Gradients and Resonances for Indoor Sound Pressure Levels

Large spatial variations in sound pressure level may occur within a house from a uniform external noise excitation. People moving within the house could be sensitive to these variations. Figure 7-37 illustrates the sound-pressure level gradient in a hallway with various combinations of open and closed doors. Noise was produced by a loudspeaker at a discrete frequency of 21 Hz. This frequency represents the low-frequency noise components from wind turbines that would propagate efficiently through buildings. When doors to Rooms A and B are both closed, there is a general decrease in the sound pressure level with distance up to the end of the hallway. When doors are opened in various combinations, the hallway pressure levels can be raised substantially. The changes in level that occur when room doors are open are similar to what might occur for side-branch resonators in a duct.

Because of the way rooms are arranged in houses, it is possible that *Helmholtz resonances* (cavity resonances) may be excited at certain frequencies, depending on the volumes of the rooms and whether doors are open or closed [Davis 1957, Ingard 1953]. Hubbard and Shepherd [1986] present results of sound-pressure-level surveys conducted inside a room during resonance. For this condition, the inside pressures were everywhere in phase and tended to maintain a uniform level. This is in contrast to the large gradients observed in the excitation of normal acoustic modes in a room [Knudsen and Harris 1978]. The latter modes are excited at frequencies for which the acoustic half-wavelengths are comparable to or less than the room dimensions, whereas Helmholtz resonance wavelengths are characteristically large compared with the room dimensions. Rooms A and B in Figure 7-37 both exhibit Helmholtz resonance behavior at an excitation frequency of 21 Hz.

#### Coupling Noise Fields in Adjacent Rooms

As sound-pressure-level gradients change in a hallway outside rooms according to whether doors are open or closed (Figure 7-37), so also do the levels inside the rooms.

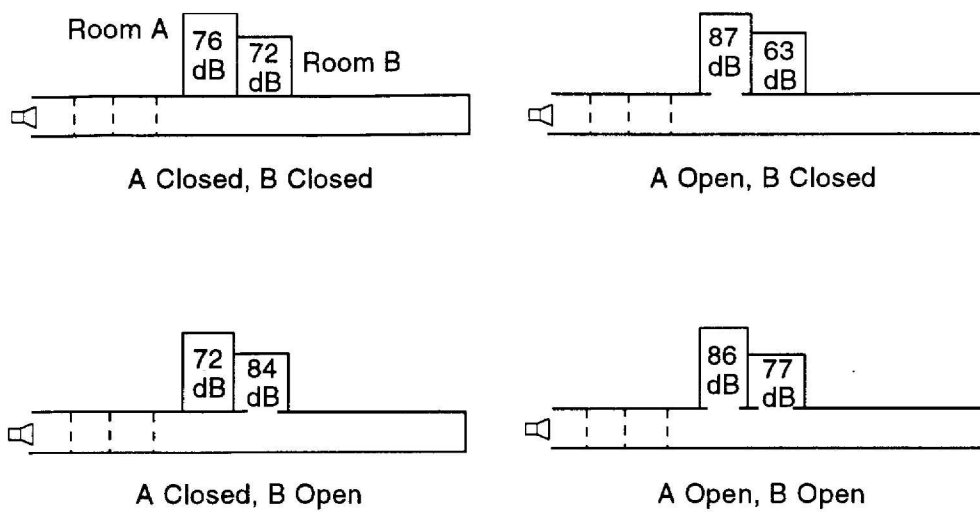


**Figure 7-38. Effect of door positions on the maximum sound pressure levels in rooms adjacent to a hallway excited by a loudspeaker at 21 Hz. [Hubbard and Shepherd 1986]**

Figure 7-38 illustrates the manner in which these changes can occur for various door positions. Variations in sound pressure level are as high as 20 dB for a steady noise input, both inside the rooms and in the hallway, as shown previously in Figure 7-37. This implies that a person might experience a change in levels of this order of magnitude at a particular location, depending on the doors, or as a function of location for a particular door arrangement. During tests, the highest sound pressure levels of Figure 7-38 could be readily heard, but the lowest levels were not audible.

Mechanical coupling between adjacent rooms can also excite acoustic resonances, as indicated by data in Hubbard and Shepherd [1986]. One wall of a test room was mechanically excited, and two response peaks were noted. One peak corresponded to the Helmholtz mode of the room, and the other was the first structural mode of the wall. Measured sound-pressure-level gradients were small in both cases.

## Perception of Building Vibrations

One of the common ways that a person senses noise-induced excitation of a house is through structural vibrations. This mode of observation is particularly significant at low frequencies, below the threshold of normal hearing.

No standards are available for the threshold of perception of vibration by occupants of buildings. Guidelines are available, however, that cover the frequency range from 0.063 to 80 Hz [Hubbard 1982, ISO 1987]. The appropriate perception data are reproduced in Figure 7-39. The hatched region in this figure shows the perception threshold data obtained in a number of independent studies. Different investigators, using different measurement techniques, subjects, and subject orientations, have obtained perception levels extending over a range of about a factor of 10 in vibration amplitude. The composite guidelines of Figure 7-39 are judged to be the best representation of the most sensitive cases from the available data on *whole-body vibration perception*.

The two small shaded regions in Figure 7-39 are from the data of Kelly *et al.* [1985]. These are estimates of levels of vibration perceived in two different houses excited by noise

from the Mod-1 HAWT. The latter data fit within the body of test data on which the composite International Standards Organization guideline is based. Therefore, they generally confirm the applicability of this guideline for structural vibrations induced by wind turbine noise.

Note that if measured vibration levels are not available they can be estimated for typical house building elements from Figure 7-36, provided the external noise excitation levels are known.

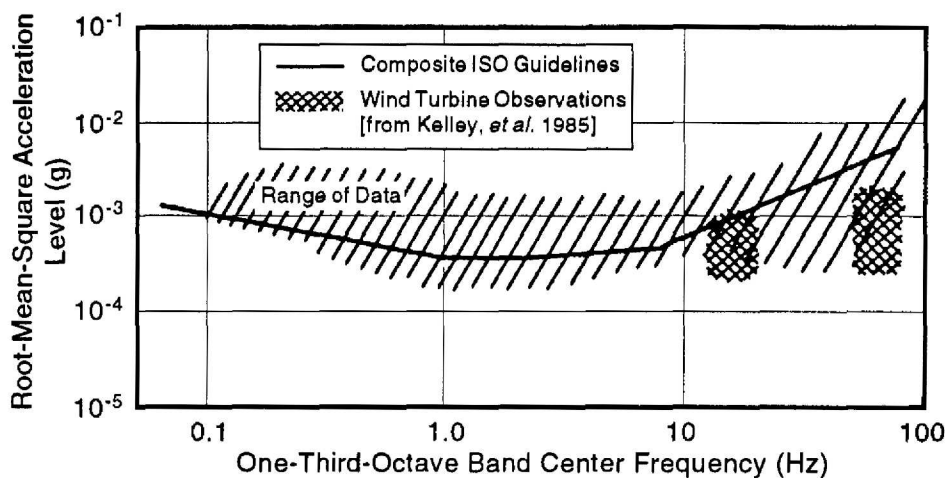


Figure 7-39. Most sensitive threshold of perception of vibratory motion. [Stephens *et al.* 1982]

## Measuring Wind Turbine Noise

Wind turbine noise is measured to define source characteristics, to provide acoustic information for environmental planning, and to validate compliance with existing ordinances. It is important to use the appropriate equipment and measurement procedures and to acquire data under appropriate test conditions. Measuring noise from wind turbine generators is particularly difficult because of the adverse effects of the wind [Andersen and Jakobsen 1983, Jakobsen and Andersen 1983]. As a result, a number of special considerations are involved in selecting measurement locations and equipment and in recording and analyzing data. This section presents some guidelines on each of these subjects.

To make meaningful comparisons of the noise outputs of different wind turbines and evaluations of environmental noise control, it is necessary to have generally accepted standards of measurement. AWEA [1988] and IEA-WECS [1988] contain the results of early work in the wind energy community to develop such standards. Both documents address significant issues in the measurement of wind turbine noise.

To interpret acoustic measurements, it is usually necessary to simultaneously record various non-acoustic quantities. Among these are wind speed and direction, ambient temperature and relative humidity, rotor speed, power output, time-of-day and date, type of terrain and vegetation, and amount of cloud cover. Atmospheric turbulence (which is often difficult to measure directly) may be inferred from this information.

### Measuring Points

Most noise measurements (other than those for research purposes) are made to characterize the radiated noise of a particular machine. This infers that all data should be obtained far enough from the machine to be in the acoustic far-field. For practical applications, the reference distance  $d_0$  illustrated in Figure 7-40 should be approximately equal to the total height of a HAWT or, in the case of a VAWT, the total height plus the rotor equatorial radius [IEA-WECS 1988]. The choice of a much greater distance may not be acceptable because of the reduced signal-to-noise ratio and because atmospheric attenuation and refraction effects can complicate interpretation of the data. To ensure the best possible signal-to-noise ratio, measurement points should be as close to the source as possible without being in the acoustic near-field.

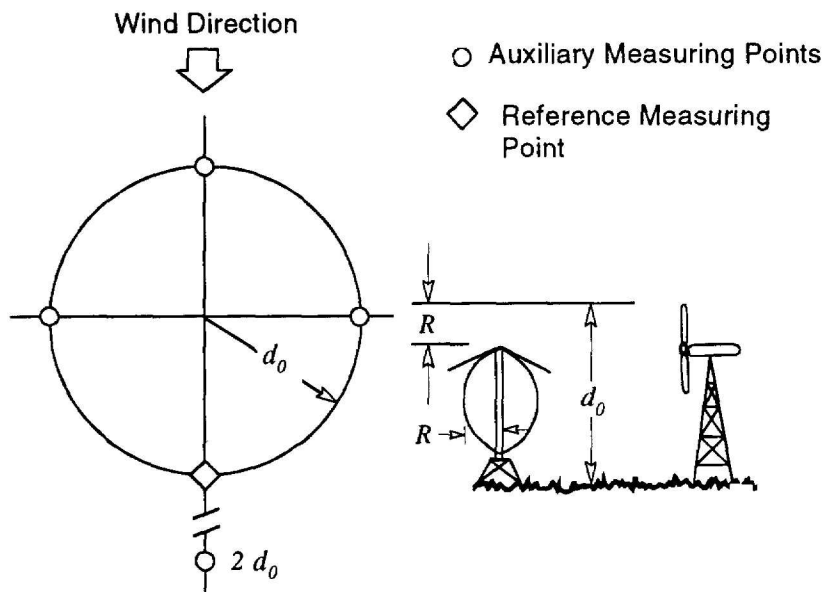


**Figure 7-40. Recommended patterns of measuring points for acoustic surveys of wind turbines. [IEA-WECS 1988]**

The number of measurement points needed can be determined by inspecting the polar diagrams in Figures 7-6 and 7-7. The aerodynamic noise sources in wind turbines are not highly directional, but the highest levels are usually in the upwind and downwind quadrants. A rather coarse azimuthal spacing seems adequate to define these aerodynamic radiation patterns around a HAWT, because they are generally symmetrical about its axis of rotation. If a particular turbine produces significant mechanical noise, however, that radiation pattern may be asymmetrical and highly directional.

### Microphone Positions

An important consideration in laying out a measurement program is defining microphone height above the ground. Placing the microphone at ear level is conceptually attractive because it should record what people hear. The disadvantage of this height is that the data are more difficult to interpret. Figure 7-41 illustrates how sound pressure level data can be affected by microphone height, and compares sound pressure levels near the ground

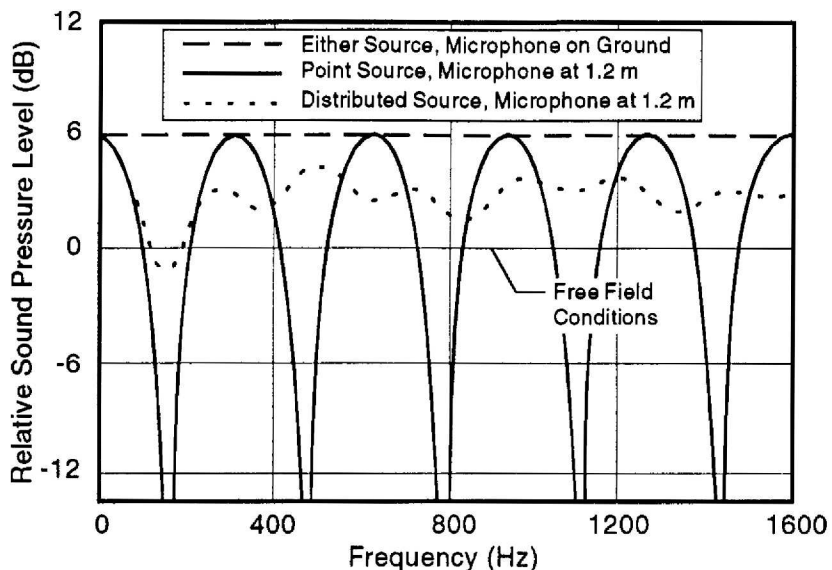


Figure 7-41. Calculated effect of microphone height on the measured noise spectra for point and distributed sources.

to results in free-field conditions (*i.e.* away from all reflecting surfaces). The solid curve represents a calculated spectrum from a point source (such as a gear box) located 20 m above hard ground, as received at a microphone position 1.2 m above ground and 40 m from the source. The peaks and valleys represent interference patterns caused by differences between the distances traveled by sounds coming directly from the source to the receiver and those reflected from the ground surface. Under ideal conditions (with no mean wind or turbulence and perfect ground reflection), the levels vary alternately from 6 dB above free-field values to very low values. For an assumed incoherent ring source with a 20-m diameter (which represents the broadband aerodynamic noises) the distributed-source curve applies. For a microphone height of 1.2 m, the variation of sound pressure level with frequency from a distributed source is less than that for a point source, but it is still significant.

A measurement at the ground surface, however, gives a constant enhancement above free-field values that is 6 dB over the entire frequency range, as indicated by the horizontal line in Figure 7-41. Thus, it is common practice to place microphones at ground level on a hard, reflecting surface (such as plywood) and then to deduct 6 dB from all measured sound pressure levels. When there are very low-frequency components to be measured, calculations suggest that microphone placement is not critical. The first dip in the spectrum occurs at a frequency well above that associated with low-frequency rotational harmonics, as shown in Figure 7-5.

#### Acoustic Instrumentation

The requirements for acoustic instrumentation are derived from the type of measurements to be performed and most directly from the frequency range of concern. For the frequency range of 20 to 10,000 Hz, standardized equipment is available for detecting, recording, and analyzing acoustic signals. A number of different microphones with flat frequency responses are available. Likewise, sound-level meters that meet existing acoustic

standards are available for direct readout or for conditioning signals before tape recording them. Either frequency-modulated or direct-record tape systems are acceptable.

For cases where the frequency range of measurements must extend below 20 Hz, some special items of equipment may be required. Although standard microphone systems can be used, their frequency response is poor at the lowest frequencies. Special microphone systems will increase signal fidelity, along with special procedures to minimize wind noise problems. A frequency-modulated tape recorder may also be required, although some direct-record systems may be acceptable if the record speed is slow and the playback speed is fast.

Because wind noise can fill much of the dynamic range of a tape recorder, it may be expedient to use dual-channel recording. In this type of recording, a high-pass filter in one of two tape recorder channels permits the simultaneous recording of low- and high-frequency segments of the same noise signal. The improved signal-to-noise ratio of the high-frequency segment enhances the signal processing.

### *Windscreen Applications*

Noise measured in the presence of wind is contaminated by various types of wind-related noises. These include *natural wind noise*, from atmospheric turbulence; *microphone noise*, caused by the aerodynamic wake of the microphone or its windscreens; *vegetation noise*, caused by nearby trees, bushes, and ground cover; and *miscellaneous wake noise*, from the aerodynamic wakes of accessories (such as a tripod) or a nearby structure.

Because of the deleterious effects of the wind, windscreens are recommended to reduce microphone noise for all measurements of wind turbine and site background noise. Commercial windscreens of open-cell polyurethane foam are usually adequate for routine measurements at or near ground level, where wind speeds are relatively low. For measurements above ground, larger windscreens of custom design may be necessary [Sutherland, Mantley, and Brown 1987]. It is essential that the acoustic insertion loss of any windscreens be either zero or known as a function of frequency, so that appropriate corrections can be made to the data.

Wind noise is a particularly severe problem at the lowest frequencies. The ambient (*i.e.*, wind-only) noise spectrum increases as frequency decreases and may submerge some low-frequency wind turbine noise components in the ambient noise at the microphone location. In such situations, customized windscreens may help reduce the low-frequency wind noise. Some special cross-correlation analysis techniques have also been applied that use measurements from pairs of microphones [Bendat and Piersol 1980].

Little can be done to reduce noise from vegetation, other than to locate microphones away from significant sources. Noise generated by the aerodynamic wakes of accessories such as tripods can often be reduced by streamlining.

### *Data Analysis*

The data analysis required depends on the types of acoustic information desired. If A-weighted data are needed, they can be obtained directly from a sound-level meter or from tape recordings and A-weighting filters. Statistical data can also be obtained directly by means of a *community noise analyzer*, or subsequently from tape recordings. Broadband data are routinely produced from one-third-octave band analysis such as that illustrated in Figure 7-8. Narrow-band analysis can be obtained with the aid of a wide range of filter bandwidths, the main requirement being that the bandwidth is small compared to frequency intervals between discrete frequency components.

## Measured Sound Power Levels

There are two important measures of the magnitude or intensity of sound that can easily be confused. These are the sound *pressure* level and the sound *power* level.

### *Sound Pressure Level*

Sound pressure level is a measure of the intensity of sound at a listener's location, and as such it is a combination of the radiated acoustic power of the noise source and the propagation of that power from the source to the listener. Thus the sound pressure level at an observer location will depend on factors such as the distance from the source, the source directivity, and the propagation path. The latter includes effects due to the atmosphere (absorption, refraction) and terrain (absorption, shielding and diffraction). As explained previously, all sound pressure levels presented in this chapter are based on root-mean-square (RMS) values of pressure and are averaged over 30 to 180 seconds, depending on the frequency bandwidth. Pressure levels in decibels are referenced to the threshold of hearing, typically defined as 20 micro-Pascals, as follows:

$$SPL = 20 \log_{10} (p / p_0) \quad (7-10)$$

where

$SPL$  = sound pressure level (dB or dBA)

$p$  = RMS acoustic pressure (Pa)

$p_0$  = reference acoustic pressure,  $2 \times 10^{-5}$  Pa

A sound pressure level can be measured with a microphone or microphone/meter at the listener's location. Sound pressure levels can vary considerably with location and time, because they depend not only on the generation of sound but also on its propagation. Therefore, sound pressure level alone is not a convenient parameter for assessing and comparing the acoustic outputs of wind turbines. Another measure is needed, and that is sound power level.

### *Sound Power Level*

Sound power level is a characteristic of the noise source, and as such it is independent of the environment around the source and the location of the listener. It is expressed in decibels and referenced to a power of 1 picowatt, as follows:

$$PWL = 10 \log_{10} (P_A / P_{A,0}) \quad (7-11)$$

where

$PWL$  = sound power level (W)

$P_A$  = acoustic power of the sound source (W)

$P_{A,0}$  = reference acoustic power,  $1 \times 10^{-12}$  W

The sound power level of a wind turbine is a noise characteristic of that turbine that does not depend on either the environment in which it is located or the relative location of a listener. For example, Søndergaard and Plovsing [2005] measured the sound power level of a 2 MW wind turbine situated in interior Danish waters, and found that the offshore levels were 1 dB to 3 dB above the onshore levels measured for the same model of wind turbine located on land. This difference is consistent with expected machine-to-machine variation when both are located on land.

While a sound power level of a wind turbine cannot be measured directly with a meter, it can be determined from sound pressure levels measured nearby, by assuming (a) the wind

turbine is a point noise source and (b) that its sound power spreads outward over a spherical surface. Sound power level is related to sound pressure level as follows:

$$PWL = SPL + 10 \log_{10} (a\pi R^2/A_0) + \alpha(R/100) + b \quad (7-12) \quad Q1$$

where

- $a$  = propagation shape factor
  - = 4 for spherical spreading *free-field* or above an ideally absorbing or anechoic surface
  - = 2 for hemispherical spreading above an ideally reflecting (hard) surface
- $R$  = slant distance from rotor center to microphone or meter (m)
- $A_0$  = reference area of sound source, 1 m<sup>2</sup>
- $\alpha$  = atmospheric absorption rate (dB per 100m)
- $b$  = empirical microphone correction constant (dB or dBA)
  - = -6 dB recommended for a microphone located on a ground board [IEC 1998]

Figure 7-26 illustrates the relative decrease in sound pressure levels assuming four different atmospheric absorption rates,  $\alpha$ , varying from 0 to 0.54 dB per 100m.

## Sound Power of Utility-Scale Wind Turbines

According to Howe *et al* [2007], modern wind turbines are considerably quieter than earlier versions, with some investigators finding a reduction in recent years of about 10 dB. While different models and different manufacturer's systems have their own acoustic characteristics, various investigators indicate that the sound power levels of utility-scale wind turbines are fairly consistent with the trend shown in Figure 7-42. Sound power levels of 105 dBA are typical for modern wind turbines in the 1 to 2 MW range at moderate wind speeds.

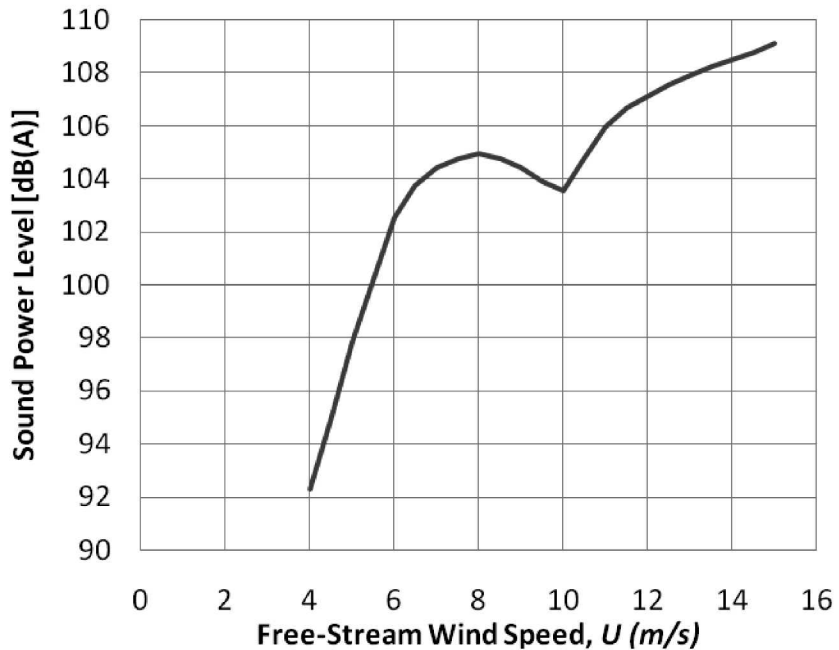


Figure 7-42. Typical sound power levels of modern 1 to 2 MW wind turbines as a function of wind speed. [Howe *et al* 2007]

## Sound Power Levels of Small-Scale Wind Turbines

Sound power levels of a variety of 3-bladed small-scale wind turbines were measured by Migliore *et al* [2003]. Rated powers of these turbines ranged from 1.0 to 100 kW, with rotor diameters of 2.1 to 19m. A graphical summary of the results of this series of acoustic tests is shown in Figure 7-43. The authors refer to these power levels as “apparent”, because they are not measured directly but inferred through the use of Equation (7-11). The constant  $a$  in this equation was set equal to 4, and the constant  $b$  was taken equal to -6dB, because sound pressure measurements were made with microphones mounted on a ground board.

Q3

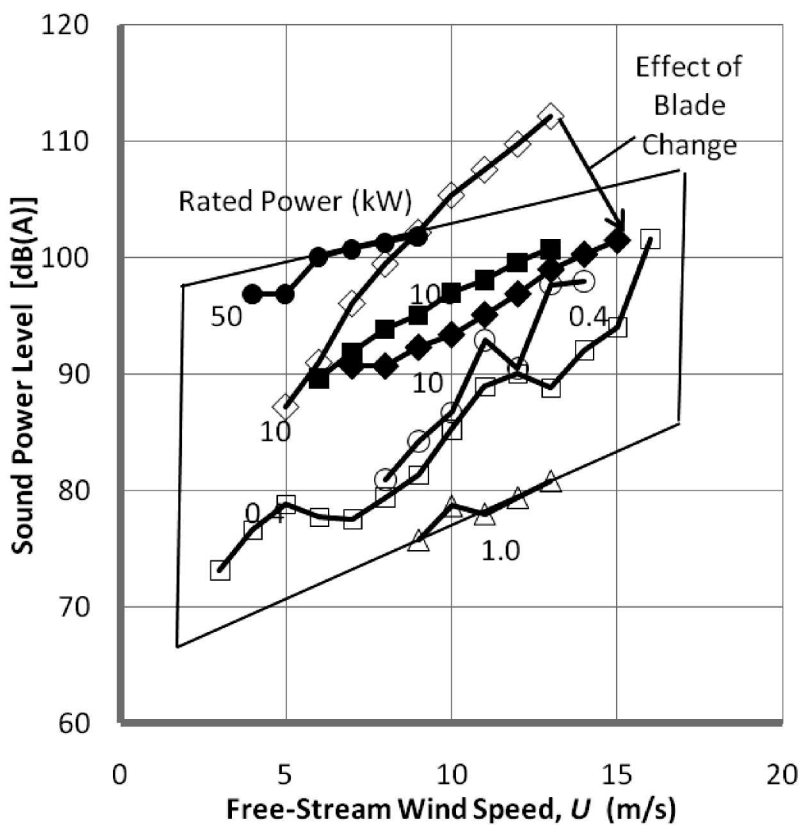


Figure 7-43. Apparent sound power levels of several small-scale, 3-bladed wind turbines with at least 6 dB(A) separation from background noise. [Migliore *et al* 2003]

Subtracting 6dB from the measured levels is an attempt to correct sound pressure levels to free-field (i.e. to remove the effect of the ground on the measurements). A ground measurement has the unique property that the direct and the ground-reflected sound are coincident and hence add “in-phase.” Thus  $a$  is set to 4 because the (measured – 6dB) sound is spreading over a free-field sphere of area  $4 \pi R^2$ , because we have removed the ground effect by subtracting 6dB. The atmospheric absorption rate  $\alpha$  was assumed to be zero.

It can be seen from Figure 7-43 that sound power levels from these small-scale wind turbines were found to increase with increasing wind speed at an average rate of about 1 dB per meter per second. Sound power also increased significantly with the rated power of the

turbines. All else being equal, one would expect a ten-fold increase in rated power to result in an approximately 10dB increase in sound power. The range of the rated powers in the figure (1-100 kW) indicates an expected 20dB range in sound power, which is approximately consistent with the measured levels.

The scale of the reduction in sound power that can be achieved by altering the shape of a rotor blade is indicated by the diamond symbols in Figure 7-43. The open diamonds show the sound power of the rotor with blades of the original design that was found to be quite noisy in higher winds. The closed diamonds indicate the much lower sound power coming from the redesigned blades on the same wind turbine. At wind speeds from 10 to 15 m/s, sound power was reduced 12 to 15 dB by the blade design change.

## Sound Sources on Wind Turbines

Acoustic tests have been conducted on an operating intermediate-scale wind turbine to determine the specific locations from which sound power is emitted. Oerlemans *et al* [2005] conducted a detailed series of noise measurements on a pitch-controlled, three-bladed *GAMESA G58* wind turbine, which has a rotor diameter of 58 m, a tower height of 53.5 m, and a rated power of 850 kW. Using an elliptical array of 152 microphones



**Figure 7-44.** Noise sources measured on a Gamesa G58 850 kW wind turbine by means of a microphone array on the platform in the foreground. The downward-moving blades emit the majority of the noise, as indicated by the sound power contours whose range is 12 dB. [Oerlemnes 2005]

1 mounted on a wooden platform on the ground, these researchers were able to obtain a profile  
2 of the noise sources on the operating turbine.

3 Figure 7-44 shows a downwind view of the test turbine onto which contours of down-  
4 ward-radiated noise levels have been projected, both from the blades and from the nacelle.  
5 The range of power levels on these contours is 12dB. The most striking phenomenon is  
6 that practically all downward radiated blade noise (as measured by the microphone array  
7 on the platform in the foreground) is produced during the downward movement of the  
8 blades. Since the range of the contours shown is 12 dB, this means that the downward-  
9 radiated noise produced during the upward movement of a blade (on the left of the tower)  
10 is at least 12 dB less than during its downward movement on the right of the tower.

11 Referring to Figure 7-14, the noise emission pattern illustrated in Figure 7-44  
12 indicates that trailing edge noise is the leading source of broadband noise from this rotor.  
13 Furthermore, it can be seen that the majority of the blade noise is produced by the outboard  
14 section of the blades, but not by the very tip in this blade design. The authors note that for a  
15 different observer location the pattern of sound emission will be different. For example, an  
16 observer located further away would “see” noise being generated over the full-blade  
17 rotation, not just over one side as indicated in this figure.

18 A second important observation is that the noise from the blades clearly dominates  
19 the noise from the nacelle. The difference between the overall sound pressure levels from  
20 the nacelle and those from the blades was found to increase with increasing wind speed,  
21 from about 8 dB(A) at 6 m/s to about 11 dB(A) at 10 m/s.

## 24 Survey of Community Response to Wind Turbine Noise

25 Studies of the reactions of nearby residents to the sight and sound of wind power stations  
26 have been conducted as part of the planning and zoning approval processes. One of  
27 the most detailed is a recent study in the Netherlands sponsored by the European Union  
28 [van den Berg *et al* 2008]. The study population was selected from all residents in the Neth-  
29 erlands living within 2.5 km from a wind turbine. As the study emphasized modern wind  
30 power stations, wind turbines were selected with a rated power of 500 kW or more and one  
31 or more turbines within 500 m from the first. Excluded were wind turbines that were erect-  
32 ed or replaced in the year preceding the survey. Residents lived in the countryside with or  
33 without a busy road close to the turbine(s), or in built-up areas (villages, towns). Excluded  
34 were residents in mixed and industrial areas. The survey was conducted by mail.

35 The sound level at the residents' dwellings was calculated according to the international  
36 ISO standard for sound propagation, the almost identical Dutch legal model, and a simple  
37 (non-spectral) calculation model. The indicative sound level used was the sound level when  
38 the wind turbines operated at a wind speed of 8 m/s in the daytime, at high but not maximum  
39 power. Respondents were exposed to levels of wind turbine sound between 24 and 54 dB(A)  
40 and wind turbines at distances from 17 m to 2.1 km. The angular elevations of the largest  
41 wind turbines ranged from 2 degrees to 79 degrees, with an average value of 10 degrees.  
42 Wind turbines occupied about 2% of the space above the horizon, on average.

## 45 Summary of the Main Conclusions of the Survey

### 46 With Respect to Hearing Wind Turbines

- 47 - Not having wind turbines visible from the dwelling and high levels of background  
48 (road traffic) sound decreased the probability of hearing wind turbine sound, though  
49 the influence of background sound was found to be small.

- Wind turbines were perceived as louder when the wind was blowing from the wind-turbine towards the dwelling and less loud vice versa.
- Wind turbines were perceived as louder when the wind was strong and less loud with a weak or no wind. However, more respondents thought it was louder than less loud at night, even though wind speeds were lower at night, on average.

#### With Respect to Annoyance from Wind Turbine Sound

- Of the potential exposures from wind turbines, noise was the most annoying.
- The most common description of annoying wind turbine sound was swishing; annoyance was more probable for respondents who gave this description than for those who did not.
- Benefiting economically from wind turbines decreased the probability of being annoyed by wind turbine sound.
- Location near a main road (in comparison with a built-up area) decreased the probability of being annoyed by wind turbine sound.
- Although the presence of background sound from road traffic made wind turbine sound less noticeable, higher levels of background sound did not reduce the probability of being annoyed.
- Annoyance with wind turbine noise was associated with a negative attitude towards wind turbines in general and the perceived negative visual impact of wind turbines on the landscape.

#### With Respect to Other Health Effects Associated with Wind Turbines

- The risk for sleep interruption by noise was higher at levels of wind turbine sound pressure levels above 45 dB(A) and lower at levels below 30 dB(A).
- Annoyance with wind turbine noise was associated with complaints of psychological distress, stress, difficulties in falling asleep, and sleep interruption.

## References

- American National Standards Institute (ANSI), 1978, *Method for the Calculation of the Absorption of Sound in the Atmosphere*, ANSI SI.26, New York: Acoustical Society of America.
- American Wind Energy Association (AWEA), 1988, *Standard Performance Testing of Wind Energy Conversion Systems*, Standard AWEA 1.2-1988, Washington, DC: American Wind Energy Association.
- Andersen, B., and J. Jakobsen, 1983, *Noise Emissions from Wind Turbine Generators: A Measurement Method*, Danish Acoustical Institute Technical Report No. 109, Lyngby, Denmark: Danish Academy of Technical Sciences.
- Bendat, J. S., and A. G. Piersol, 1980, *Engineering Applications of Correlation and Spectral Analysis*, New York: John Wiley and Sons.
- Brooks, T. F., and T. H. Hodgson, 1980, *Prediction and Comparison of Trailing Edge Noise Using Measured Surface Pressures*, Preprint 80-0977, American Institute of Aeronautics and Astronautics.

- 1 Brooks, T. F., and M. A. Marcolini, 1986, "Airfoil Tip Vortex Formation Noise," *AIAA Journal*, Vol. 24, No. 2.
- 2
- 3
- 4 Daigle, G. A., T. F. W. Embleton, and J. E. Piercy, 1986, "Propagation of Sound in the  
5 Presence of Gradients and Turbulence Near the Ground," *Journal of the Acoustical  
6 Society of America*, Vol. 79, No.3.
- 7
- 8 Davis, D. D. Jr., 1957, "Acoustical Filters and Mufflers," *Handbook of Noise Control*,  
9 C. M. Harris, ed., New York: McGraw Hill.
- 10
- 11 George, A. R., 1978, "Helicopter Noise State-of-the-Art," *Journal of Aircraft*, Vol. 15,  
12 No. 11: pp. 707-711.
- 13
- 14 George, A. R., and S. T. Chou, 1984, "Comparison of Broadband Noise Mechanisms,  
15 Analyses, and Experiments on Rotors," *Journal of Aircraft*, Vol. 21.
- 16
- 17 Glegg, S. A. L., S. M. Baxter, and A. G. Glendinning, 1987, "The Prediction of Broadband  
18 Noise for Wind Turbines," *Journal of Sound and Vibration*, Vol. 118, No. 2:  
19 pp. 217-239.
- 20
- 21 Greene, G. C., and H. H. Hubbard, 1980, *Some Effects of Non-Uniform Inflow on the  
22 Radiated Noise of a Large Wind Turbine*, NASA TM-8183, Hampton, Virginia: NASA  
23 Langley Research Center.
- 24
- 25 Greene, G. C, 1981, "Measured and Calculated Characteristics of Wind Turbine Noise,"  
26 *Proceedings, Wind Turbine Dynamics Conference*, R. W. Thresher, ed., NASA  
27 CP-2185, DOE Publication CONF-810226, Cleveland, Ohio: NASA Lewis Research  
28 Center, pp. 355-362.
- 29
- 30 Grosveld, F. W., 1985. "Prediction of Broadband Noise from Horizontal Axis Wind  
31 Turbines," *AIAA Journal of Propulsion and Power*, Vol. 1, No. 4.
- 32
- 33 Hawkins, J. A., 1987, *Application of Ray Theory to Propagation of Low Frequency Noise  
34 from Wind Turbines*, NASA CR-178367, Hampton, Virginia: NASA Langley Research  
35 Center.
- 36
- 37 Howe, B. W. Gastmeier, and N. McCabe, 2007, "Wind Turbines and Sound: Review and  
38 Best Practice Guidelines," report submitted by HGC Engineering, Mississauga,  
39 Ontario, to the Canadian Wind Energy Association, Ottawa, Ontario.
- 40
- 41 Hubbard, H. H., 1982, "Noise Induced House Vibrations and Human Perceptions," *Noise  
42 Control Engineering Journal*, Vol. 19, No. 2.
- 43
- 44 Hubbard, H. H., and K. P. Shepherd, 1982, *Noise Measurements for Single and Multiple  
45 Operation of 50-kW Wind Turbine Generators*, NASA CR-166052, Hampton, Virginia:  
46 NASA Langley Research Center.
- 47
- 48 Hubbard, H. H., and K. P. Shepherd, 1984, *The Effects of Blade Mounted Vortex  
49 Generators on the Noise from a Mod-2 Wind Turbine Generator*, NASA CR-172292,  
50 Hampton, Virginia: NASA Langley Research Center.
- 51

- Hubbard, H. H., and K. P. Shepherd, 1986, *The Helmholtz Resonance Behavior of Single and Multiple Rooms*, NASA CR-178173, Hampton, Virginia: NASA Langley Research Center.
- Hubbard, H. H., and K. P. Shepherd, 1988, *Wind Turbine Acoustics Research Bibliography with Selected Annotation*, NASA TM 100528, Hampton, Virginia: NASA Langley Research Center.
- IEA-WECS, 1988, *Recommended Practices for Wind Turbine Testing 4. Acoustics Measurement of Noise Emission from Wind Turbines*, International Energy Agency Programme for Research and Development on Wind Energy Conversion Systems, Second Edition, Bromma, Sweden: Aeroacoustical Research Institute of Sweden.
- Ingard, U., 1953, "On the Theory and Design of Acoustic Resonators," *Journal of the Acoustical Society of America*, Vol. 25, No. 6.
- International Standards Organization (ISO), 1971, *Community Response to Noise*, ISO Standard R 1996-1971 (E), New York: Acoustical Society of America.
- International Standards Organization (ISO), 1987, *Evaluation of Human Exposure to Whole Body Vibration - Part 2: Human Exposure to Continuous and Shock-Induced Vibrations in Buildings (1 Hz to 80 Hz)*, Draft ISO Standard 2631-2.2, New York: Acoustical Society of America.
- Jakobsen, J., and B. Andersen, 1983, *Wind Noise Measurements of Wind-Generated Noise from Vegetation and Microphone System*, Danish Acoustical Institute Technical Report No. 108, Lyngby, Denmark: Danish Academy of Technical Sciences.
- Kelley, N. D., R. R. Hemphill, and D. L. Sengupta, 1981, "Television Interference and Acoustic Emissions Associated with the Operation of the Darrieus VAWT," *Proceedings, 5th Biennial Wind Energy Conference and Workshop, Vol. I*, I. E. Vas, ed., SERI/CP-635-1340, Golden, Colorado: National Renewable Energy Laboratory, pp. 397-413.
- Kelley, N. D., R. R. Hemphill, and H. E. McKenna, 1982, "A Comparison of Acoustic Emission Characteristics of Three Large Wind Turbine Designs," *Proceedings, Inter-Noise '82*, New York: Noise Control Foundation.
- Kelley, N.D., H.E. McKenna, R.R. Hemphill, C.L. Etter, R.C. Garrelts, and N.C. Linn, 1985, *Acoustic Noise Associated with the MOD-1 Wind Turbine: Its Source, Impact and Control*, SERITR-635-1166, Golden Colorado: National Renewable Energy Laboratory.
- Kelley, N.D., H.E. McKenna, E. W. Jacobs, R.R. Hemphill, and N.J. Birkenheuer, 1987, *The MOD-2 Wind Turbine: Aeroacoustical Noise Sources, Emissions, and Potential Impact*, SERI/TR-217-3036, Golden, Colorado: National Renewable Energy Laboratory.
- Knudsen, V.O., and CM. Harris, 1978, *Acoustical Designing in Architecture*, New York: American Institute of Physics.
- Lowson, M.V., Nov. 1970, "Theoretical Analysis of Compressor Noise," *Journal of the Acoustical Society of America*, Vol. 47, No. 1 (Part 2).

- 1 Lunggren, S., 1984, *A Preliminary Assessment of Environmental Noise from Large WECS,*  
2 *Based on Experience from Swedish Prototypes*, FFA TN 1984-48, Stockholm, Sweden:  
3 Aeronautical Research Institute of Sweden.
- 4 Martinez, R., S.E. Widnall, and W.L. Harris, 1982, *Prediction of Low Frequency Sound*  
5 *from the MOD-1 Wind Turbine*, SERI TR-635-1247, Golden, Colorado: National  
6 Renewable Energy Laboratory.
- 7 Meijer, S. and I. Lindblad, 1983, *A Description of Two Methods for Calculation of Low*  
8 *Frequency Wind Turbine Noise, Including Applications for the Swedish Prototype*  
9 *WECS Maglarp*, FFA TN 1983-31, Stockholm, Sweden: Aeronautical Research Institute  
10 of Sweden.
- 11 Migliore, P., J. van Dam, and A. Huskey, 2003, "Acoustic Tests of Small Wind Turbines,"  
12 NREL/CP-500-34662, National Renewable Energy Laboratory, Golden, Colorado.
- 13 Oerlemans, S., and B. Méndez López, 2005, "Acoustic Array Measurements on a Full-  
14 Scale Wind Turbine," NLR-TP-2005-336, National Aerospace Laboratory NLR.
- 15 Pearson, K.S., and R.L. Bennett, 1974, *Handbook of Noise Ratings*, NASA CR-2376,  
16 Hampton, Virginia: NASA Langley Research Center.
- 17 Piercy, J.E., T.F.W. Embleton, and L.C. Sutherland, 1977, "Review of Noise Propagation in  
18 the Atmosphere," *Journal of the Acoustical Society of America*, Vol. 61, No. 6.
- 19 Piercy, J.E., and T.F.W. Embleton, 1979, "Sound Propagation in the Open Air," *Handbook*  
20 *of Noise Control 2nd Edition*, edited by CM. Harris, New York: McGraw Hill.
- 21 SAE, 1966, *Method for Calculating the Attenuation of Aircraft Ground to Ground Noise*  
22 *Propagation During Takeoff and Landing*, SAE Aerospace Information Report AIR  
23 923, Warrendale, Pennsylvania: Society of Automotive Engineers.
- 24 Schlinker, R.H, and R.K. Amiet, 1981, *Helicopter Rotor Trailing Edge Noise*, NASA  
25 CR-3470, Hampton, Virginia: NASA Langley Research Center.
- 26 Sears, W.R., 1941, "Some Aspects of Non-Stationary Airfoil Theory and Its Practical  
27 Application," *Journal of Aerospace Sciences*, Vol. 8, No. 3.
- 28 Shepherd, K. P., and H. H. Hubbard, 1981, *Sound Measurements and Observations of the*  
29 *Mod-OA Wind Turbine Generator*, NASA-CR-165752, Hampton, Virginia; NASA  
30 Langley Research Center.
- 31 Shepherd, K. P., and H. H. Hubbard, 1983, *Measurements and Observations of Noise from*  
32 *a 4.2 Megawatt (WTS-4) Wind Turbine Generator*, NASA CR-166124, Hampton,  
33 Virginia: NASA Langley Research Center.
- 34 Shepherd, K. P., and H. H. Hubbard, 1984, *Acoustics of the Mod-0/5A Wind Turbine Rotor*  
35 *with Two Different Ailerons*, NASA CR-172427, Hampton, Virginia: NASA Langley  
36 Research Center.
- 37 Shepherd, K. P., 1985, *Detection of Low Frequency Impulsive Noise from Large Wind*  
38 *Turbine Generators*, NASA CR-172511, Hampton, Virginia: NASA Langley Research  
39 Center.

- Shepherd, K. P., and H. H. Hubbard, 1985, *Sound Propagation Studies for a Large Horizontal Axis Wind Turbine*, NASA CR-172564, Hampton, Virginia: NASA Langley Research Center.
- Shepherd, K. P., and H. H. Hubbard, 1986, *Prediction of Far Field Noise from Wind Energy Farms*, NASA CR-177956, Hampton, Virginia: NASA Langley Research Center.
- Shepherd, K. P., W. L. Willshire, Jr., and H. H. Hubbard, 1988, *Comparisons of Measured and Calculated Sound Pressure Levels around a Large Horizontal Axis Wind Turbine Generator*, NASA TM 100654, Hampton, Virginia: NASA Langley Research Center.
- Søndergaard, B. and B. Plovsing, 2005, "Noise from Offshore Wind Turbines," Danish Ministry of the Environment Report, Environmental Project No. 1016 2005.
- Stephens, D. G., 1979, "Developments in Ride Quality Criteria," *Noise Control Engineering Journal*, Vol. 12, No. 1.
- Stephens, D. G., K. P. Shepherd, H. H. Hubbard, and F. W. Grosveld, 1982, *Guide to the Evaluation of Human Exposure to Noise from Large Wind Turbines*, NASA M-83288, Hampton, Virginia: NASA Langley Research Center.
- Sutherland, L. C, R. Mantey, and R. Brown, 1987, *Environmental and Cumulative Impact of Noise from Major Wind Turbine Generator Developments in Alameda and Riverside Counties — Literature Review and Measurement Procedure Development*, WR87-8, El Segundo, California: Wylie Laboratories.
- Thomson, D. W., 1982, *Analytical Studies and Field Measurements of Infrasound Propagation at Howard's Knob, North Carolina*, SERI/TR-635-1292, Golden, Colorado: National Renewable Energy Laboratory.
- Thomson, D. W., 1982, "Noise Propagation in the Earth's Surface and Planetary Boundary Layers," *Proceedings, Internoise-82 Conference*, New York: Noise Control Foundation.
- Viterna, L. A., 1981, *The NASA-LeRC Wind Turbine Sound Prediction Code*, NASA CP-2185, Cleveland, Ohio: NASA Lewis Research Center.
- Wehrey, M. C, T. H. Heath, R. J. Yinger, and S. F. Handschin, 1987, *Testing and Evaluation of a 500-kW Vertical Axis Wind Turbine*, AP-5044, Palo Alto, California: Electric Power Research Institute.
- Willshire, W. L. Jr., and W. E. Zorumski, 1987, "Low Frequency Acoustic Propagation in High Winds," *Proceedings, Noise-Con 87 Conference*, New York: Noise Control Foundation.
- van den Berg, F., E. Pedersen, J. Bouma, R. Bakker, 2008, WINDFARMperception: Visual and Acoustic Impact of Wind Turbine Farms on Residents," FP6-2005-Science-and-Society-20 Specific Support Action Project No. 044628 Final Report.



# **Author Query Form**

**(Queries are to be answered by the Author)**

## **Chapter 7 - ASME Wind Turbine**

The following queries have arisen during the typesetting of your manuscript. Please answer these queries.

<b>Query Marker</b>	<b>Query</b>	<b>Reply</b>
Q1	Equation number was renumbered. Please check if correct.	
Q2	Please check if a descriptor is missing here.	
Q3	Please check if equation 11 here needs to be renumbered.	

Thank you very much.